Deep-sea Research Part Ii-topical Studies In Oceanography
March 2016, Volume 125-126 Pages 163-176
https://doi.org/10.1016/j.dsr2.2015.03.007
https://archimer.ifremer.fr/doc/00421/53261/

Surface nitrate utilization in the Bering sea since 180 kA BP: Insight from sedimentary nitrogen isotopes

Riethdorf Jan-Rainer [1, 2], Thibodeau Benoit [2, 3], Ikehara Minoru [4], Nuernberg Dirk [2], Max Lars [5], Tiedemann Ralf [5], Yokoyama Yusuke [1, 6, *]

[1] Univ Tokyo, Atmosphere & Ocean Res Inst, Dept Ocean Floor Geosci, 5-1-5 Kashiwanoha, Kashiwa, Chiba 2778564, Japan.
[2] Helmholtz Ctr Ocean Res Kiel GEOMAR, Wischhofstr 1-3, D-24148 Kiel, Germany.
[3] Univ Tokyo, Atmosphere & Ocean Res Inst, Dept Chem Oceanog, 5-1-5 Kashiwanoha, Kashiwa, Chiba 2778564, Japan.
[4] Kochi Univ, Ctr Adv Marine Core Res, B200 Monobe Nankoku, Kochi 7838502, Japan.
[5] Alfred Wegener Inst Polar & Marine Res, Handelshafen 12, D-27570 Bremerhaven, Germany.
[6] Japan Agcy Marine Earth Sci & Technol, Inst Biogeosci, 2-15 Natsushimacho, Yokosuka, Kanagawa 2370061, Japan.

* Corresponding author : Yusuke Yokoyama, email address : yokoyama@aori.u-tokyo.ac.jp

jan.riethdorf@gmail.com ; bthibodeau@geomar.de ; ikehara@kochi-u.ac.jp ; dnuernberg@geomar.de ; Lars.Max@awi.de ; Ralf.Tiedemann@awi.de

Abstract :

We present high-resolution records of sedimentary nitrogen (delta N-15(bulk)) and carbon isotope ratios (delta C-13(bulk)) from piston core S0201-2-85KL located in the western Bering Sea. The records reflect changes in surface nitrate utilization and terrestrial organic matter contribution in submillennial resolution that span the last 180 kyr. The delta N-15(bulk) record is characterized by a minimum during the penultimate interglacial indicating low nitrate utilization (similar to 62-80%) despite the relatively high export production inferred from opal concentrations along with a significant reduction in the terrestrial organic matter fraction (m(terr)). This suggests that the consumption of the nitrate pool at our site was incomplete and even more reduced than today (similar to 84%). delta N-15(bulk) increases from Marine Isotope Stage (MIS) 5.4 and culminates during the Last Glacial Maximum, which indicates that nitrate utilization in the Bering Sea was raised during cold intervals (MIS 5.4, 5.2, 4) and almost complete during MIS 3 and 2 (similar to 93-100%). This is in agreement with previous hypotheses suggesting that stronger glacial stratification reduced the nutrient supply from the subeuphotic zone, thereby increasing the iron-to-nutrient ratio and therefore the nitrate utilization in the mixed surface layer. Large variations in delta N-15(bulk) were also recorded from 180 to 130 ka BP (MIS 6), indicating a potential link to insolation and sea-level forcing and its related feedbacks. Millennial-scale oscillations were observed in delta N-15(bulk) and delta C-13(bulk) that might be related to Greenland interstadials.

Keywords : Bering Sea, Quaternary, Nitrogen isotopes, Nitrate utilization

1. Introduction

The polar oceans are thought to have been more stratified during past glacial periods and the breakdown of stratification in the Southern Ocean during interglacials has been suggested as a potential control mechanism for the glacial-interglacial cycles in atmospheric carbon dioxide (CO_2) (for a review see Sigman et al., 2010). Recent studies have found supporting evidence that past variations in stratification/ventilation also occurred in the subarctic North Pacific with implications for ocean-atmosphere

gas exchange (Jaccard et al., 2005, 2010; Brunelle et al., 2007, 2010; Galbraith et al., 2008a; Okazaki et al., 2010, 2012; Chikamoto et al., 2012; Menviel et al., 2012; Rella et al., 2012; Jaccard and Galbraith, 2013; Max et al., 2014).

The modern subarctic North Pacific is characterized by a permanent halocline due to a low-salinity surface layer that limits the exchange of nutrients between the surface and subsurface and prevents the formation of deep water masses (e.g., Warren, 1983; Haug et al., 1999; Emile-Geay et al., 2003). At the same time high marine productivity makes this area a net sink for atmospheric CO_2 (Honda et al., 2002; Takahashi et al., 2002b). However, the efficiency of the biological pump in the high-nutrient, low-chlorophyll (HNLC) regions of the subarctic North Pacific is reduced due to iron limitation (e.g., Tsuda et al., 2003), which results in incomplete nitrate utilization.

Sedimentary records from the North Pacific and its marginal seas consistently show reduced contents of biogenic opal and barium, $CaCO_3$, and organic carbon during past glacial periods, indicating reduced biological export production (e.g., Gorbarenko et al., 2002; Narita et al., 2002; Kienast et al., 2004; Nürnberg and Tiedemann, 2004; Jaccard et al., 2005, 2010; Okazaki et al., 2005a; Shigemitsu et al., 2007, 2008; Riethdorf et al., 2013a). Restricted marine productivity both in the North Pacific and in the Antarctic sector of the Southern Ocean is attributed to (i) light limitation due to extensive sea-ice coverage (Elderfield and Rickaby, 2000), or (ii) to enhanced stratification of the upper water column that suppressed nutrient supply to the euphotic zone (Francois et al., 1997).

Studies investigating these hypotheses applied stable nitrogen isotope ratios ($\delta^{15}N$) to provide a link to the marine nutrient cycle, but they have been mostly focused on regions not influenced by seasonal sea-ice, which has the potential to modulate biological and terrigenous fluxes. In the NW Pacific the $\delta^{15}N$ signal can be used as a proxy of surface nitrate utilization, whereas in the NE Pacific, it reflects variations in the composition of the subsurface nitrate pool (Brunelle et al., 2007; Galbraith et al., 2008a). The available reconstructions of surface nitrate utilization in the Okhotsk and Bering seas indicate that in both marginal seas enhanced stratification during glacial intervals resulted in a reduced supply of nitrate to the surface and a more complete

utilization of surface nitrate because of the continued iron supply from atmospheric deposition (i.e., higher iron-to-nitrate ratio), thereby explaining the low glacial productivity (e.g., Brunelle et al., 2007, 2010; Kim et al., 2011; Khim et al., 2012).

For the Bering Sea, recent studies have found indications for millennial-scale oscillations in export production and terrigenous matter supply, which might be connected to changes in stratification and/or sea-ice influence (Gorbarenko et al., 2005, 2010b; Kim et al., 2011; Riethdorf et al., 2013a; Schlung et al., 2013). However, most of the available records of $\delta^{15}N$ are located in the southern Bering Sea and therefore not necessarily influenced by seasonal sea-ice. Moreover, the records are restricted to ~120 ka BP and do not allow for a comparison between the glacial terminations, which due to the large amplitude of climate and environmental changes are considered important periods for the understanding of the carbon cycle (e.g., Yokoyama and Esat, 2011). Especially for Marine Isotope Stage 6 (MIS 6), which in the Okhotsk Sea environment is characterized by rather extreme glacial ice conditions with significantly increased accumulation rates of ice-rafted debris (IRD) (Nürnberg et al., 2011), no records of $\delta^{15}N$ are available.

Here, we present isotope geochemical records from a supposedly sea-ice influenced site in the poorly studied western Bering Sea for the last 180 kyr in high-resolution employing sedimentary carbon and nitrogen isotope ratios to reconstruct changes in the contribution of terrestrial organic matter and surface nitrate utilization, respectively. Our results, for the first time, provide information on nitrate utilization in the Bering Sea beyond 120 ka BP and expand the hypothesis of glacial-interglacial stratification changes to cold and warm intervals. Moreover, our record suggests that millennial-scale climate oscillations occurred in the Bering Sea which might be connected to Greenland interstadials.

2. Study area

The Bering and Okhotsk seas are marginal seas of the North Pacific, separated from by the Aleutian and Kurile islands, respectively. They are bounded by the coasts of eastern Siberia, the Kamchatka Peninsula and/or western Alaska. Wide and shallow

continental shelf areas are found in the northern Okhotsk and in the northern and eastern Bering Sea (Figure 1).

With respect to surface circulation, waters from the North Pacific are transported westward along the Aleutian islands by the Alaskan Stream and enter the Bering Sea via the Aleutian passes. There, the Bering Slope Current (BSC) and the East Kamchatka Current (EKC) form boundary currents (Stabeno et al., 1999). Surface outflow is directed into the Arctic Ocean through the shallow (~50 m) Bering Strait, whereas surface and deeper waters are transported back into the NW Pacific through the deeper straits, mainly Kamchatka Strait (Figure 1). The EKC and the Oyashio current flow southward and represent western boundary currents of the North Pacific subpolar gyre. The Kurile straits provide entrance and exit pathways to the Okhotsk Sea.

Major climatic and oceanographic characteristics of the North Pacific realm are the strong seasonality in sea surface temperatures (SST) and sea-ice formation, the permanent halocline, and a pronounced oxygen minimum zone (OMZ). In the Bering Sea sea-ice is present from September until July reaching its maximum distribution during March/April (Tomczak and Godfrey, 1994; Niebauer et al., 1999). The sea-ice formation is related to the interaction of the Siberian High and the Aleutian Low, which results in the advection of cold Arctic air masses, subsequent cooling of the sea surface, and strong winter mixing (Stabeno et al., 1999). Sea-ice is considered as an important transport agent of terrigenous matter in the Okhotsk and Bering seas (Nürnberg and Tiedemann, 2004; Nürnberg et al., 2011; Riethdorf et al., 2013a). Geochemical results indicate that sediments on the eastern Bering Sea shelf and in the Meiji Drift in the NW Pacific are supplied from Yukon–Bering Sea sources (VanLaningham et al., 2009; Asahara et al., 2012; Nagashima et al., 2012). Based on these results Riethdorf et al. (2013a) proposed that terrigenous matter entrained into sea-ice by tidal pumping, suspension freezing, and beach-ice formation, was transported from the eastern Bering Sea shelf to the location studied in this paper, although a contribution by suspension load carried by the BSC could not be excluded.

Although sea-ice formation and according brine rejection in the northern Okhotsk Sea drive the modern ventilation of North Pacific Intermediate Water (NPIW) (e.g., Yasuda, 1997; Yamamoto et al., 2001), the source of NPIW might have shifted to the Bering Sea in the past (Matsumoto et al., 2002; Ohkushi et al., 2003; Tanaka and Takahashi, 2005; Rella et al., 2012), where it nowadays resides at the depth of the 26.8 potential density (σ_Θ) surface in ~200-400 m (Roden, 1995; Macdonald et al., 2001). The OMZ is found beneath the NPIW with minimum dissolved oxygen concentrations of ~15-20 µmol kg^{-1} at ~900-1100 m (Roden, 2000; Lehmann et al., 2005).

In the Bering Sea, high marine productivity is observed, which is mainly associated with shelf areas (e.g., Springer et al., 1996; Stabeno et al., 1999) and dominated by diatoms. Major biological fluxes occur during spring/summer (mainly diatoms) and late summer/early fall (coccolithophores and planktonic foraminifera) (Takahashi et al., 2002a). Nutrients are consumed during the productive seasons and returned from the subsurface by winter mixing. Although winter mixing supplies nutrients from the subsurface into the euphotic zone, near-surface nutrients are not completely consumed by phytoplankton during the productive seasons. Therefore, the western Bering Sea studied here, as well as the central eastern and western parts of the subarctic North Pacific are HNLC regions with perennially high surface nitrate concentrations (e.g., Tyrrell et al., 2005) (Figure 1). As extensively discussed in Brunelle et al. (2007, 2010) changes in the extent of surface nitrate utilization can be reconstructed using records of $\delta^{15}N$, if the underlying assumptions include a constant isotope effect for nitrate assimilation and little or no changes in the $\delta^{15}N$ of the source nitrate. There is evidence for the northward propagation of ^{15}N-enriched nitrate from the eastern tropical North Pacific along coastal North America (Liu and Kaplan, 1989; Altabet et al., 1999; Kienast et al., 2002; Sigman et al., 2003). Hence, paleoceanographic interpretations of sedimentary $\delta^{15}N$ have to consider changes in the $\delta^{15}N$ of the subsurface nitrate pool.

3. Material and methods

This study is based on 18.13 m-long piston core SO201-2-85KL (referred to as 85KL hereafter) recovered during R/V Sonne expedition SO201 KALMAR Leg 2 in 2009 (Dullo et al., 2009) from Shirshov Ridge, western Bering Sea (57°30.30'N, 170°24.77'E, 968 m water depth; Figure 1). Sediments from this core mainly consist of terrigenous siliciclastic material bound to the clay- and silt-fractions, but layers of diatomaceous ooze are repeatedly intercalated. Carbonate preservation is poor and at best sporadic, and no sediments younger than 7.5 ka BP were recovered.

3.1 Bulk sedimentary analyses (TOC, TN, $\delta^{13}C_{bulk}$, $\delta^{15}N_{bulk}$)

Total organic carbon (TOC) and total nitrogen (TN) concentrations, as well as sedimentary stable carbon ($\delta^{13}C_{bulk}$) and nitrogen ($\delta^{15}N_{bulk}$) isotope ratios were determined downcore (>9.1 ka BP) every 5 cm from a total of 357 bulk sediment samples. About 25 mg of freeze-dried, hand-ground (agate mortar) sediment was weighed into Ag capsules, acidified with 100 µl hydrochloric acid (3N) to remove inorganic carbon, and dried in a desiccator filled with phosphorus pentoxide and sodium hydroxide. To ensure complete combustion, the Ag capsules were subsequently wrapped into Sn capsules. TOC, TN, $\delta^{13}C_{bulk}$, and $\delta^{15}N_{bulk}$ were determined at the Center for Advanced Marine Core Research, Kochi University, using a Flash EA 1112 Series elemental analyzer (EA; Thermo Fisher Scientific, USA) coupled with a Delta Plus Advantage isotope ratio mass spectrometer (IRMS; Thermo Fisher Scientific, USA) via a Conflo III interface (He carrier). Stable isotope results are reported in conventional δ-notation and referenced to the Vienna PeeDee Belemnite (VPDB) standard and to atmospheric nitrogen. Molar TN/TOC ratios were corrected for inorganic nitrogen compounds based on a linear regression between TOC and TN following Goñi et al. (1998) (referred to as molar N/C ratios hereafter; Figure 2). Analytical precision (1σ) was determined from two different standards (L-Alanine, n = 58; Sulfanilamide, n = 60) and was <2% RSD (relative standard deviation) for TOC, <5% RSD for TN, ±0.01 for molar N/C ratio, ±0.14‰ for $\delta^{13}C_{bulk}$, and ±0.29‰ for $\delta^{15}N_{bulk}$. Reproducibility of the samples, determined from replicates (1σ, n = 14), was ±0.01 wt.% for TOC and TN, ±0.01 for molar N/C ratio, ±0.11‰ for

212 $\delta^{13}C_{bulk}$, and ±0.86‰ for $\delta^{15}N_{bulk}$. This rather high value for $\delta^{15}N_{bulk}$, being significantly
213 higher than instrumental precision, might be related to sample inhomogeneity and
214 potential alteration of the sedimentary organic matter during pre-analysis acid
215 treatment (Brodie et al., 2011a, 2011b).

216

217 **3.2 Age model**

218 The stratigraphic framework of 85KL is described in detail in Max et al. (2012) and
219 Riethdorf et al. (2013a). Briefly, X-ray fluorescence (XRF) and spectrophotometric
220 (color b*) core logging data were correlated to the $\delta^{18}O$ records of the NGRIP ice
221 core (NGRIP members, 2004; GICC05 timescale, Rasmussen et al., 2006) and the
222 Sanbao stalagmites (Wang et al., 2008). This approach was validated by benthic
223 $\delta^{18}O$ stratigraphy, magnetostratigraphy, accelerator mass spectrometry (AMS)
224 radiocarbon dating of planktonic foraminifera, and intercore correlations to
225 neighbouring sediment cores. Linear sedimentation rates vary between 4 and 23 cm
226 kyr^{-1} (average of ~12 cm kyr^{-1}), which translates into a submillennial time-resolution
227 for our reconstructions.

228

229 **3.3 Existing data**

230 For comparison we used logging data and geochemical results reflecting changes in
231 export production and terrigenous matter supply already available for core 85KL.
232 Method details are given elsewhere (Max et al., 2012; Riethdorf et al., 2013a,
233 2013b). In summary, light and color reflectance were measured directly after core
234 recovery every 1 cm using a Minolta CM 508d hand-held spectrophotometer and
235 converted into *Commission Internationale de l'Éclairage* (CIE) *L**, *a**, and *b** color
236 space. XRF scanning for elements Al through to Ba was performed at 1 cm sampling
237 resolution using the Avaatech XRF core scanner at Alfred Wegener Institute for Polar
238 and Marine Research, Bremerhaven. Molybdate-blue spectrophotometry was used to
239 determine biogenic opal concentrations (after Müller and Schneider, 1993), and
240 concentrations of $CaCO_3$ were calculated from the difference of total carbon (TC) and
241 TOC previously determined using a Carlo Erba CNS analyzer (model NA-1500) at

GEOMAR, Kiel. The relative amount of siliciclastics was calculated by subtracting the sum of $CaCO_3$, TOC, and opal concentrations from a total of 100 wt.%. Records of XRF Ca/Ti log-ratios, XRF Br count rates (in counts per second, cps), and color b* correlated with $CaCO_3$ (R^2 = 0.65), TOC (R^2 = 0.64), and opal (R^2 = 0.61), respectively. This finding is in agreement with other studies linking biogenic $CaCO_3$ with normalized XRF records of Ca (Jaccard et al., 2005), TOC with biophilic Br (Ziegler et al., 2008), and opal and organic matter content with color b* (Debret et al., 2006).

3.4 Reconstruction of export production

The use of $CaCO_3$, TOC, and opal to reconstruct changes in export production is subject to specific restrictions. $CaCO_3$, especially in the North Pacific, is influenced by carbonate dissolution and might be more indicative of changes in the bottom water calcite saturation state (e.g. Jaccard et al., 2005). With respect to TOC, it is necessary to discriminate between marine and terrestrial carbon sources. The most often used proxy for reconstructions of paleo-export production in the North Pacific realm is biogenic opal (e.g. Kienast et al., 2004).

In paleoceanography, fluxes are usually reconstructed using accumulation rates rather than proxy concentrations. However, for the North Pacific and Bering Sea several studies provide evidence for the similar evolution of concentration and accumulation records of biogenic components (e.g. Crusius et al., 2004; Brunelle et al., 2007, 2010). Here, we used dry bulk density measurements (Riethdorf et al., 2013a) to calculate bulk mass accumulation rates (AR Bulk, in g cm^{-2} kyr^{-1}), as well as proxy accumulation rates for $CaCO_3$, TOC, opal, and siliciclastics. The result is shown in Figure 3, clearly demonstrating that sedimentation at Site 85KL is dominated by siliciclastic input. Overall, concentrations of the biogenic components are low, but opal concentrations and opal accumulation rates show a positive linear relationship (R^2 = 0.49). We therefore assume in this paper that at Site 85KL concentrations of opal and color b* logging data are related to export production.

4. Results

4.1 Export production and terrigenous matter supply

In general, concentrations of $CaCO_3$, TOC, and opal, as well as their approximating logging data show increased values during warm intervals (MIS 5.5, 5.3, 5.1, and 1) and Greenland interstadials (GI), but low values during cold intervals (MIS 6, 5.4, 5.2, 4, and 2) and Greenland stadials (GS) (Figure 4; Riethdorf et al., 2013a). Because of sedimentary dilution, the proxy records reflecting terrigenous matter supply (%Siliciclastics, XRF data of Al) have an inversed shape with respect to the records reflecting export production. Our EA-IRMS-based TOC results are in excellent agreement with those of Riethdorf et al. (2013a) and in higher temporal resolution extend the respective record by ~30 kyr into MIS 6. The temporal evolution of TOC recorded during MIS 6 strongly corresponds to that observed in color b*, and, to a lesser degree, in XRF Ca/Ti log-ratios and Br count rates (Figure 4). With respect to TOC concentrations, MIS 6 is characterized by a strong variability within the range of ~0.4 to ~1.7 wt.%, showing several short-lived oscillations and highest concentrations during ~156-137 ka BP.

4.2 $\delta^{13}C_{bulk}$, $\delta^{15}N_{bulk}$, molar N/C ratios, and estimation of the terrestrial organic matter fraction (m_{terr})

Values for $\delta^{13}C_{bulk}$ (of TOC) and for $\delta^{15}N_{bulk}$ (of TN) ranged from -25.4 to -21.9‰ and from 1.7 to 7.5‰, respectively, and molar N/C ratios varied between 0.04 and 0.11 (Table 1; Figures 5 and 6). In general, $\delta^{13}C_{bulk}$ and molar N/C ratios are more positive during warm intervals (MIS 5.5, 5.3, 5.1, 3, and 1) and show pronounced, but short-lived maxima during GI, which especially for $\delta^{13}C_{bulk}$ exceed analytical precision and reproducibility. The cold intervals (MIS 5.4, 5.2, and 4) and some GS are characterized by decreases in both proxies. A different temporal evolution is recorded for $\delta^{15}N_{bulk}$. The base of core 85KL shows $\delta^{15}N_{bulk}$ values of ~5-6‰, which is followed by a sharp decrease at ~172 ka BP to values of ~2-3‰ (Figure 6). Subsequently, $\delta^{15}N_{bulk}$ again increases until another sudden drop of ~3‰ characterizes the transition from MIS 6 to 5.5 (Termination II). During the last

interglacial $\delta^{15}N_{bulk}$ remained low at ~3‰ but it decreased even further to minimum values of 1.7‰ at the beginning of cold MIS 5.4. After MIS 5.4, a long-term trend toward higher values that continues into the early Holocene is observed. In between, increasing values were recorded during cold MIS 5.2 and 4, whereas $\delta^{15}N_{bulk}$ decreased (MIS 5.1) or remained almost constant (MIS 5.3 and 3) during warm stages. The transition from MIS 2 to 1 (Termination I) is characterized by local minima (~4-5‰) during the cold phases of Heinrich Stadial 1 (HS1; 18.0-14.7 ka BP, Sarnthein et al., 2001) and the Younger Dryas (YD; 12.9-11.7 ka BP, Blockley et al., 2012), and by an intercalated pronounced maximum during the Bølling-Allerød warm phase (B/A; 14.7-12.9 ka BP, Blockley et al., 2012) (up to 6.8‰). Subsequent to the YD, $\delta^{15}N_{bulk}$ continuously increased until highest values of 7.5‰ were recorded during the early Holocene (~10.1 ka BP). Notably, the $\delta^{15}N_{bulk}$ record also features short-lived maxima during GI, which, however, must be considered insignificant with respect to reproducibility.

Assuming that the geochemical and isotopic sedimentary composition represents a mixture of marine and terrestrial organic matter we applied a linear mixing model to estimate the fraction of terrestrial-derived organic matter (m_{terr}) using hypothetical endmember compositions. We therefore followed the results of Walinsky et al. (2009). This approach has recently been applied to a sediment core from the northern Gulf of Alaska (Addison et al., 2012). Our Holocene samples lie within the ranges reported by Smith et al. (2002) for surface sediment samples from the southeastern Bering Sea shelf, whereas our glacial samples compare to terrigenous particulate organic matter (POM) from the Yukon River (Guo and Macdonald, 2006) (Figure 5). Accordingly, we assume that the most likely organic matter sources for our site are marine phytoplankton ($\delta^{13}C$: -22 to -20‰; $\delta^{15}N$: >5‰; molar N/C ratio: 0.10 to 0.15), soil ($\delta^{13}C$: -26.5 to -25.5‰; $\delta^{15}N$: 0 to 1‰; molar N/C ratio: 0.08 to 0.10), and vascular plant detritus (VPD; $\delta^{13}C$: -27 to -25‰; $\delta^{15}N$: 0 to 1‰; molar N/C ratio: 0 to 0.05) (Meyers, 1994; McQuoid et al., 2001; Geider and La Roche, 2002; Smith et al., 2002; Guo et al., 2004; Gaye-Haake et al., 2005; Guo and Macdonald, 2006; Walsh et al., 2008, and references therein) (Figure 5; Table 2). With the influence of soil considered insignificant, m_{terr} was calculated as:

$$m_{terr} = (A_{sample} - A_{mar}) / (A_{terr} - A_{mar}) \quad \textit{(Eq. 1)}$$

In Equation 1 A refers to the $\delta^{13}C_{bulk}$ or molar N/C ratio of the sample and the respective average values for the assumed marine and terrestrial endmember composition summarized in Table 2. We preferred using molar N/C over C/N ratios, because mixing lines based on C/N are reported to underestimate the fraction of terrestrially derived organic carbon (Perdue and Koprivnjak, 2007). This approach resulted in similar values but in part different temporal evolutions of the respective m_{terr} records, which is attributed to the low variability in molar N/C ratios. m_{terr} varied between ~10% and ~90% with average values of ~40-50% (Table 1). It was lowest during warm intervals (MIS 5.5, 5.3, 5.1, 3, and 1) and GI, when marine productivity was high. Reductions of up to 50% occurred during the transitions from cold to warm intervals, whereas pronounced but short-lived increases of ~20% seem to correspond to GS (Figure 6). In the discussion we refer to m_{terr} derived from $\delta^{13}C_{bulk}$.

5. Discussion

5.1 The $\delta^{15}N_{bulk}$ signal and potential alteration

$\delta^{15}N_{bulk}$ values reflect the isotopic signature of the export flux of organic matter plus any secondary alteration of this signal during sinking and burial (e.g., Galbraith et al., 2008b; Robinson et al., 2012, and references therein). Hence, interpretation of variations in the $\delta^{15}N_{bulk}$ record must consider changes in (i) the isotopic composition of the subsurface nitrate pool, which is controlled by nitrogen fixation by diazotrophic bacteria and by denitrification, (ii) the degree of nitrification and surface nitrate utilization, and (iii) secondary alteration.

Nitrate is the primary nitrogen source for marine phytoplankton, which preferentially incorporates isotopically light (^{14}N-enriched) nitrate (Pennock et al., 1996; Waser et al., 1998). In the Bering Sea the source nitrate is supplied to the surface from below the euphotic zone with a modern value ($\delta^{15}N_{nitrate}$) of ~5.5‰ (Lehmann et al., 2005), which is slightly higher than the global deep ocean average of ~5‰ because of denitrification in the North Pacific (Sigman et al., 2000, Brunelle et al., 2007). Nitrogen fixation results in $\delta^{15}N_{nitrate}$ values that are isotopically light and close to that

of air (0‰; Carpenter et al., 1997), and it is the main reason for the low $\delta^{15}N$ values of nitrate and sinking detritus in the tropical/subtropical ocean basins (e.g., Somes et al., 2010). Water column denitrification occurs under low dissolved oxygen concentrations (<5 µmol l^{-1}; Codispoti et al., 2001) and results in a ^{15}N-enriched nitrate pool (Barford et al., 1999). In this respect, $\delta^{15}N$ might also reflect redox conditions in the past with higher values during bottom water suboxia (Galbraith et al., 2004; Kashiyama et al., 2008; Jaccard and Galbraith, 2012; Robinson et al., 2012). Today, water column denitrification is mainly observed in the Arabian Sea, the eastern tropical North Pacific, and in the eastern tropical South Pacific. Thus, the export of ^{15}N-enriched waters might result in a shift toward higher $\delta^{15}N_{nitrate}$, as observed along coastal North America in the subarctic NE Pacific (Liu and Kaplan, 1989; Altabet et al., 1999; Kienast et al., 2002; Sigman et al., 2003). However, modern dissolved oxygen concentrations at Site 85KL lie above the denitrification threshold.

Results from benthic foraminiferal assemblages from the same site (Ovsepyan et al., 2013) suggest oxidizing conditions in the surface sediment layer from MIS 3 to the Last Glacial Maximum (LGM), but oxygen-depleted conditions during the mid-B/A and early Holocene. This is in agreement with Kim et al. (2011) who for Site PC23A reported on a dominance of oxic benthic foraminiferal species during MIS 2 and 3, but on dominantly dysoxic species during the B/A, early Holocene, and GI. These observations and our proxy records for export production indicate the presence of mostly oxic bottom waters and strongly reduced export of organic matter during most of the past 180 kyr, arguing against a significant impact of water column denitrification on $\delta^{15}N_{bulk}$. Over the last 180 kyr, one can expect a slightly higher $\delta^{15}N$ of nitrate during warm stages because of the greater extent of denitrification in the North Pacific. The isotopic impact of such increased denitrification during warm stages is thought to be relatively equal to the one observed today (~0.5‰: Lehmann et al., 2005). This shift toward heavier $\delta^{15}N$ is opposite to the expected isotopic effect of decreased nitrate utilization during interglacials. Thus, the relatively small increase in $\delta^{15}N_{bulk}$ during warm stages (~0.5‰) should not mask the larger isotopic variation expected from the change in nitrate utilization (Brunelle et al., 2007, and references therein). Thus, we are confident that the observed variations in our $\delta^{15}N_{bulk}$ can be

used to assess relative changes in the utilization of nitrate in the Bering Sea surface water, except for periods where dysoxia were locally present. During phases of locally enhanced export production and oxygen-depleted bottom water conditions, as recorded during the B/A and the early Holocene, as well as during GI, denitrification might have resulted in a shift toward heavier $\delta^{15}N_{bulk}$ values. Because we can not isolate this signal in our record, our nitrate utilization estimates for these periods might not be accurate due to potential changes in the $\delta^{15}N$ signature of the source nitrate

Nitrate utilization is incomplete in the modern subarctic North Pacific and in the Bering Sea. Accordingly, the isotopic value of the export flux of organic matter ($\delta^{15}N_{export}$) is lighter than that of $\delta^{15}N_{nitrate}$ (Altabet and Francois, 1994; Sigman et al., 1999; Needoba et al., 2003; Galbraith et al., 2008a). The difference between $\delta^{15}N_{nitrate}$ and $\delta^{15}N_{export}$ is primarily controlled by the nitrate utilization and decreases as it becomes more complete and in most of the global ocean the difference is zero due to almost complete utilization (Altabet et al., 1999; Thunell et al., 2004). We can calculate $\delta^{15}N_{export}$ for the expected integrated organic nitrogen export at Site 85KL assuming Rayleigh fractionation kinetics (Altabet and Francois, 1994; Mariotti et al., 1981) after:

$$\delta^{15}N_{export} = \delta^{15}N_{nitrate} + f / (1 - f)\ \varepsilon \ln (f) \qquad \textit{(Eq. 2)}$$

In Equation 2 f is the fraction of unutilized nitrate (i.e., $[NO_3^-]_{summer} / [NO_3^-]_{winter}$) and ε is the isotope effect for nitrate incorporation by phytoplankton, which was assumed to be constant at ~5‰ for simplification (Brunelle et al., 2007, 2010). Using a modern average for f of 0.16 (84% utilization), estimated from WOA 2009 surface nitrate concentrations (Garcia et al., 2010), gives $\delta^{15}N_{export}$ = ~3.8‰ for our site, which is 1.7‰ lower than the modern $\delta^{15}N_{nitrate}$. Unfortunately, no coretop $\delta^{15}N_{bulk}$ results are available for verification at our site.

Alternatively, secondary alteration (preferential loss of organic nitrogen, leakage of ammonium into pore waters, ammonium absorption into clay minerals, winnowing/size fractionation) might have raised the modern coretop $\delta^{15}N$ value. In general, however, alteration of the $\delta^{15}N_{bulk}$ from that of the sinking flux is not

considered to have a considerable influence in organic-rich sediments from high-accumulation regions with low contributions of inorganic nitrogen compounds (for a review see Robinson et al., 2012). Core 85KL has rather high average TOC concentrations (~0.9 wt.%), whereas TIN is low at ~0.017 wt.% (Figure 2a), and the relationship between TN and $\delta^{15}N_{bulk}$ is only weak (R^2 = 0.24; Figure 2b), which argues against alteration. Moreover, in comparison with other Bering Sea records using $\delta^{15}N$ as a proxy for nitrate utilization (Brunelle et al., 2007, 2010; Kim et al., 2011; Schlung et al., 2013) our $\delta^{15}N_{bulk}$ record generally shows a similar evolution (Figure 7). Notably, at our study site $\delta^{15}N_{bulk}$ values >5.5‰ were mainly recorded during Termination I, which, in accordance with the previously mentioned studies is more likely attributed to enhanced deglacial water column denitrification.

Finally, there might have been influence from terrestrial nitrogen, since our estimates for m_{terr} suggest significant average contributions (~40-50%) of terrestrial organic matter in Shirshov Ridge sediments. In this respect, variations in $\delta^{15}N_{bulk}$ might reflect changes in the supply of terrestrial nitrogen. However, for the estimation of m_{terr} we assumed that the $\delta^{15}N_{bulk}$ of terrestrial organic matter is lower than that of marine organic matter. If there was considerable influence from terrestrial nitrogen we would expect a strong positive relationship between molar N/C ratios and $\delta^{15}N_{bulk}$, which is not observed (R^2 = 0.10). Accordingly, although Site 85KL is characterized by overall high m_{terr} values with a strong downcore variability, there seems to have been no significant influence of m_{terr} on the $\delta^{15}N_{bulk}$ signal, which might be explained by an only low fraction of terrestrial nitrogen. We therefore consider the influence of secondary alteration and contamination from terrestrial nitrogen on the $\delta^{15}N_{bulk}$ signal as insignificant and in the following discuss variations in $\delta^{15}N_{bulk}$ by means of changes in surface nitrate utilization.

5.2 Cold and warm intervals of the past 180 kyr

At Site 85KL, glacial periods, specifically cold intervals (MIS 6, 5.4, 5.2, and 4 to 2), were characterized by significantly reduced export production and enhanced terrigenous matter supply (Riethdorf et al., 2013a; Figure 4), which is in agreement

with other studies from the subarctic North Pacific (e.g., Kienast et al., 2004; Jaccard et al., 2005), the Okhotsk Sea (e.g., Narita et al., 2002; Nürnberg and Tiedemann, 2004; Okazaki et al., 2005b; Nürnberg et al., 2011), and the Bering Sea (e.g., Okazaki et al., 2005a; Brunelle et al., 2007; Kim et al., 2011). This is supported by our reconstruction of m_{terr} indicating an average terrestrial organic matter fraction of ~40-50%, which is significantly reduced only during warm intervals. Today, the organic matter in Bering Sea sediments is dominantly of marine origin (Méheust et al., 2013). The glacial terrigenous matter source of Bering Sea sediments is under debate, but there are indications that they originate from source rocks drained by the Yukon River (VanLaningham et al., 2009), and/or from sea-ice rafting in the NE Bering Sea (Riethdorf et al., 2013a).

For the Bering and Okhotsk seas the outlined observations were explained by enhanced sea-ice influence and stronger stratification of the upper water column during cold climate conditions restricting marine productivity (Nürnberg and Tiedemann, 2004; Brunelle et al., 2007, 2010; Kim et al., 2011; Khim et al., 2012; Riethdorf et al., 2013a). This restriction results from the extended sea-ice season and coverage and the subsequent limitation of light availability and vertical mixing (nutrient supply), but temperature limitation is likely to have played an additional role. An extended Bering Sea sea-ice coverage during cold phases is supported by reconstructions from diatom assemblages (Katsuki and Takahashi, 2005) and from the diatom-derived, highly branched isoprenoid sea ice biomarker (IP_{25}) (Max et al., 2012).

Records of sedimentary and diatom-bound $\delta^{15}N$ imply enhanced surface nitrate utilization as a result of stronger upper water column stratification in the Bering Sea, especially during MIS 3 and 2 (Brunelle et al., 2007, 2010; Kim et al., 2011). Similar observations are reported for the Okhotsk Sea (Brunelle et al., 2010; Khim et al., 2012) and the subarctic NW Pacific (Galbraith et al., 2008a; Brunelle et al., 2010), indicating that these regions were not always HNLC. This shift towards higher $\delta^{15}N$ in MIS 3 is, however, not observed at IODP Site U1340 at the northeastern flank of Bowers Ridge (Schlung et al., 2013). Instead, a sharp decrease in $\delta^{15}N_{bulk}$ was recorded at this site at ~55 ka BP, which might be related to local stratification changes, or to the influence of turbidites that are reported to compromise records

recovered from that area (Nakatsuka et al., 1995). Our $\delta^{15}N_{bulk}$ results are in accordance with the former Bering Sea studies confirming enhanced nitrate utilization during cold intervals, but they seem to reveal a more complex development of stratification and for the first time provide information for MIS 6.

At the base of core 85KL (~180-173 ka BP), early MIS 6 is characterized by high $\delta^{15}N_{bulk}$ values indicating almost complete nitrate utilization, when export production was reduced, but maintained. Relatively high $\delta^{15}N_{bulk}$ during MIS 6 were also recorded at Okhotsk Sea sites GGC27 (Brunelle et al., 2010) and GC9A (Khim et al., 2012), as well as at ODP Site 882 and at Site MD01-2416 (Galbraith et al., 2008a). Hence, low insolation and weak seasonal contrasts most probably caused a prolonged sea-ice season, extended sea-ice coverage, and suppressed vertical mixing. At ~172 ka BP, when Northern Hemisphere summer insolation had a local maximum, a sharp decrease in $\delta^{15}N_{bulk}$ implies a sudden drop in nitrate utilization (from ~100% to ~50-70%) in the Bering Sea (Figure 6). At the same time export production was increased, whereas m_{terr} decreased. This might be explained by a shortened sea-ice season, reduced sea-ice coverage, and enhanced winter mixing due to stronger seasonal contrasts, which increased the nutrient supply from the subeuphotic zone.

Accordingly, we speculate that changes in nitrate utilization are strongly affected by insolation forcing and a feedback by sea-ice processes that drive the extent of vertical mixing during winter, as well as the input of terrestrial organic matter. Dominant climate control via insolation has already been proposed for the Okhotsk Sea (Gorbarenko et al., 2010a, 2012). The long-term increase in nitrate utilization after ~172 ka BP until Termination II, which is also observed at the Okhotsk Sea and NW Pacific sites (Figure 7), as well as the long-term increase from MIS 5.4 until Termination I might be explained by increasingly fostered stratification (i.e. a reduction in the supply of nutrients into the euphotic zone), which is finally subject to a 'breakdown' during the deglaciations. It is beyond the scope of this paper to decipher the underlying causes of this deglacial breakdown, but increasing insolation resulting in a reduced sea-ice season and strengthened winter mixing, is a likely contributing factor.

519 The observation that the strongest maxima in Northern Hemisphere summer
520 insolation, mainly those of warm intervals (MIS 5.5, 5.3, 5.1, and 1), are reflected by
521 maxima in export production (Figure 4), minima in m_{terr}, and decreasing or constant
522 $\delta^{15}N_{bulk}$ (Figure 6), supports the view that insolation changes affect nutrient-limited
523 marine productivity by a feedback in sea-ice processes and winter mixing. It is also in
524 agreement with previously published concepts proposed to explain glacial-interglacial
525 changes in the Okhotsk (Seki et al., 2004; Okazaki et al., 2005b; Khim et al., 2012)
526 and Bering seas (Nakatsuka et al., 1995; Kim et al., 2011). When applying Equation
527 2, our $\delta^{15}N_{bulk}$ record indicates increasing nitrate utilization during cold MIS 5.4 (from
528 ~50 to ~90%), MIS 5.2 (from ~90 to ~100%), and MIS 4 (from ~80 to ~93%), and
529 almost complete utilization during MIS 3 and 2 (~93-100%). On the other hand,
530 decreasing or constant nitrate utilization was recorded during warm MIS 5.5 (from
531 ~97 to ~62%), MIS 5.3 (~90%), and MIS 5.1 (from ~100 to ~80%). This suggests that
532 stratification was fostered during cold intervals, but weakened during warm intervals
533 due to the processes outlined above.

534 The low glacial $\delta^{15}N_{bulk}$ values of ~2-3‰ at the beginning of MIS 5.4, of ~3.5-4.5‰ at
535 the beginning of MIS 4, and the concurrent increases in m_{terr} (Figure 6) might be
536 explained (i) by a higher contribution of (^{15}N-depleted) terrestrial organic matter, or (ii)
537 by stronger vertical mixing. We disregard the first possibility, because we already
538 discarded the potential effect of terrestrial nitrogen on the $\delta^{15}N_{bulk}$ signal (Section
539 5.1). Stronger vertical mixing in the Bering Sea during MIS 5.4 and 4 might be related
540 to the increased formation and/or ventilation of intermediate waters as inferred from
541 neodymium isotope ratios by Horikawa et al. (2010). The authors suggested that sea-
542 ice formation and according brine rejection led to the subduction of surface waters to
543 intermediate depths. Enhanced formation of sea-ice, acting as the transport agent for
544 terrestrial organic matter would be in accordance with this assumption and explain
545 the higher m_{terr} values. Other studies support the idea of well-ventilated intermediate
546 waters in the Bering Sea and North Pacific during glacial times (Ohkushi et al., 2003;
547 Itaki et al., 2009; Kim et al., 2011) and during severe stadial episodes (Rella et al.,
548 2012). The enhanced formation and/or ventilation of intermediate waters at the end
549 of MIS 6 and during the LGM implied by the record of Horikawa et al. (2010) is not
550 reflected in our $\delta^{15}N_{bulk}$ record, which rather suggests strong stratification during that

551 time. However, these observations are not necessarily contradictory, since
552 intermediate waters could have been formed outside the still-stratified Bering Sea. In
553 fact, recent reconstructions of past ventilation changes in the subarctic North Pacific
554 using radiocarbon-derived ventilation ages in combination with epibenthic stable
555 carbon isotope ratios point to the Okhotsk Sea as the source region of intermediate
556 waters during HS1 and the YD (Max et al., 2014).

557 In addition to insolation forcing, sea-level changes might have influenced the extent
558 of stratification in the Bering Sea. Today, the only shallow (~50 m) Bering Strait
559 allows for oceanic communication between the North Pacific and the N Atlantic.
560 During glacial times the closed Bering Strait prevented the flux of relatively fresh
561 waters into the Atlantic, which is thought to have affected the Atlantic meridional
562 overturning circulation (Hu et al., 2010). Lower glacial sea-level is also likely to have
563 reduced the inflow of Alaskan Stream waters into the Bering Sea (Gorbarenko et al.,
564 2005; Tanaka and Takahashi, 2005). As suggested by relative sea-level
565 reconstructions (e.g., Waelbroeck et al., 2002; Yokoyama and Esat, 2011), the
566 Bering Strait was closed during MIS 6 and in between MIS 4 to 2 until ~12-11 ka BP
567 (Keigwin et al., 2006) (Figure 6). Our $\delta^{15}N_{bulk}$ values indicate almost complete nitrate
568 utilization during late MIS 6 (~150-130 ka BP) and during MIS 3 and 2 as a result of
569 strong stratification. During this time a closed Bering Strait is likely to have fostered
570 stratification due to the pooling of the relatively fresh waters within the Bering Sea,
571 which would have resulted in a strengthened pycnocline. Support for this view and for
572 fresher glacial conditions in the Bering Sea comes from diatom and radiolarian
573 assemblages (Sancetta, 1983; Katsuki and Takahashi, 2005; Tanaka and Takahashi,
574 2005). Notably, during MIS 3 and 2 the $\delta^{15}N_{bulk}$ values recorded at Shirshov Ridge
575 are on average ~1‰ lower than at Bowers Ridge Site 17JPC and ~0.5‰ lower than
576 at Site PC24A (Figure 7). This might indicate that stratification in the Bering Sea was
577 regionally different and more pronounced in the South, or that influence from
578 denitrification resulted in the heavier $\delta^{15}N$ values.

579

580

581

582 **5.3 Deglacial and interglacial conditions**

583 In our records, the deglaciations are characterized by the transition from the glacial
584 situation of pronounced stratification with almost complete nitrate utilization and low
585 export production toward the interglacial situation of reduced stratification, high
586 marine productivity, and reduced terrestrial input. Yet, Termination II and Termination
587 I show some notable differences. During Termination I our $\delta^{15}N_{bulk}$ record is
588 characterized by an initial decrease, which might correspond to the HS1 cold phase,
589 subsequent local maxima during the B/A and the early Holocene warm phases, and
590 an intercalated minimum during the YD (Figure 6). The same temporal evolution was
591 reported for sedimentary and diatom-bound $\delta^{15}N$ at Bering Sea sites 17JPC (Brunelle
592 et al., 2007, 2010) and PC24A (Kim et al., 2011). The B/A-peak, occurring
593 simultaneously with a rise in export production, is found in several other records from
594 the North Pacific realm and related to enhanced denitrification (Keigwin et al., 1992;
595 Emmer and Thunell, 2000; Ternois et al., 2001; Kienast et al., 2002; Galbraith et al.,
596 2008a; Kao et al., 2008; Brunelle et al., 2007, 2010; Addison et al., 2012; Khim et al.,
597 2012; Schlung et al., 2013).

598 Notably, m_{terr} shows a local maximum during HS1 at Site 85KL. Hence, the initial
599 decrease in $\delta^{15}N_{bulk}$ might be related to higher terrestrial input or to lower nitrate
600 utilization due to weakened stratification. However, the latter should have resulted in
601 higher export production, which is not observed at our site. This drop is not fully
602 understood and alternative explanations include changes in $\delta^{15}N_{nitrate}$, iron limitation,
603 and light limitation (Brunelle et al., 2007, 2010; Lam et al., 2013). Light limitation by
604 expanded sea-ice coverage is supported by the qualitative detection of IP_{25} in
605 western Bering Sea sediments during HS1 and the YD (Max et al., 2012).

606 During the B/A and the early Holocene our $\delta^{15}N_{bulk}$ values exceeded the modern
607 $\delta^{15}N_{nitrate}$ value, supporting an increase in denitrification. At the same time a shift
608 toward oxygen-depleted bottom water conditions is inferred from benthic foraminiferal
609 assemblages (Kim et al., 2011; Ovsepyan et al., 2013), which is in agreement with
610 the proposed expansion of the OMZ and the occurrence of laminated sediments
611 during warm intervals (e.g., Zheng et al., 2000; van Geen et al., 2003; Cook et al.,
612 2005; Kuehn et al., 2014). A recent comparison between alkenone- and Mg/Ca-

based paleotemperature estimates suggests enhanced thermal mixed-layer stratification in the western Bering Sea during the B/A (Riethdorf et al., 2013b), implying that at least some of the recorded $\delta^{15}N_{bulk}$ increase is due to stronger surface nitrate utilization. Recently, Lam et al. (2013) suggested two stepwise events starting with deep convection initialized at ~18 ka BP increasing the nutrient supply but inducing light limitation, and subsequent meltwater-induced stratification resulting in bloom conditions and leaving surface waters enriched in nutrients. The drop in $\delta^{15}N_{bulk}$ observed during the YD in hand with decreasing SSTs and the presence of IP_{25} (Max et al., 2012) argues for a similar situation as recorded during HS1.

Termination II differs from Termination I at Site 85KL in such that the $\delta^{15}N_{bulk}$ values are lower and presumably not affected by denitrification. An early deglacial $\delta^{15}N_{bulk}$ minimum at ~133 ka BP, followed by a local maximum at ~131 ka BP might hint toward analogs of the HS1 and the B/A, respectively. The subsequent drop in $\delta^{15}N_{bulk}$ into MIS 5.5 reflecting the 'breakdown' of glacial stratification is sudden and accompanied by the decrease in both, m_{terr} and bottom water oxygenation then prevailing during the penultimate interglacial (Figure 6). Notably, this drop from relatively high MIS 6 values occurred ~5 kyr before the maximum in insolation was reached, but its timing is comparable to that recorded in the NW Pacific. In the Okhotsk Sea it seems to have occurred significantly earlier at ~147-141 ka BP (Figure 7). A respective drop in $\delta^{15}N_{bulk}$ during Termination I was not recorded at Site 85KL until ~9.1 ka BP, while at Bowers Ridge sites U1340 (Schlung et al., 2013) and 17JPC (Brunelle et al., 2007) it occurred directly after the B/A maximum.

5.4 Millennial-scale oscillations

Riethdorf et al. (2013a) reported on millennial-scale oscillations in core 85KL, thought to reflect increased export production and sudden sea-ice melt, which might be connected to GI (Dansgaard-Oeschger events; e.g., Dansgaard et al., 1993). Similar observations are reported for other sediment cores from the Bering Sea (Gorbarenko et al., 2005, 2010b; Kim et al., 2011; Rella et al., 2012; Schlung et al., 2013) and the Okhotsk Sea (Gorbarenko et al., 2007, 2010a, 2012), indicating warmer SSTs, enhanced marine productivity, weak ventilation of intermediate waters, and poor

644 (dysoxic) dissolved oxygen conditions during interstadials. NE Pacific sediments
645 related to GI are in part laminated and suggested to reflect phases of weak
646 ventilation of NPIW and fluctuations in the strength of the OMZ (Behl and Kennett,
647 1996; Cannariato and Kennett, 1999; Hendy and Kennett, 2000, 2003). Results of
648 Ortiz et al. (2004) from a core off Baja California implied that elevated marine
649 productivity was caused by enhanced nutrient flux to surface waters.

650 In the Bering Sea higher interstadial $\delta^{15}N_{bulk}$ values were explained by Kim et al.
651 (2011) by increased marine productivity as a result of reduced sea-ice influence and
652 a strengthened BSC. They also suggested that stronger inflow of water masses from
653 the Gulf of Alaska (Gorbarenko et al., 2005) resulted in enhanced nutrient supply to
654 Bering Sea surface waters. Schlung et al. (2013) attributed higher $\delta^{15}N_{bulk}$ and
655 concurrent minima in planktonic $\delta^{13}C$ to amplified local upwelling of subsurface
656 nitrate rather than to increased nitrate utilization. Our data show short-lived maxima
657 in $\delta^{15}N_{bulk}$ and concurrent minima in m_{terr} during some, but not all, GI (1, 7, 8, 12, 17-
658 20), and during MIS 6 (at ~133, ~148, and ~173 ka BP) when export production was
659 high (Figure 6). The opposite pattern was recorded when export production was low
660 during some GS (2, 7, 18, 20) and also during MIS 6 (at ~151, ~157, and ~170 ka
661 BP). Despite the low reproducibility of our $\delta^{15}N_{bulk}$ results our data support the view of
662 increased interstadial marine productivity which led to stronger utilization of the
663 available nitrate in a still stratified upper water column. During interstadials warmer
664 SSTs most probably resulted in less sea-ice influence and reduced supply of
665 terrestrial organic matter. Conversely, during stadials strengthened sea-ice formation
666 and coverage is likely to have restricted marine productivity, led to enhanced
667 terrestrial organic matter supply to Bering Sea sediments, and resulted in better
668 ventilation of NPIW, potentially making the Bering Sea a proximate source of this
669 water mass as suggested by Rella et al. (2012).

670

671 **6. Summary**

672 We determined TN, TOC, $\delta^{13}C_{bulk}$ and $\delta^{15}N_{bulk}$ in a core from the western Bering Sea
673 in high-resolution to reconstruct changes in surface nitrate utilization (stratification)
674 over the last 180 kyr. A linear endmember model was applied to assess the

675 contributions of marine- and terrestrial-derived organic matter. Besides the expected
676 difference between glacial and interglacial conditions reported for the subarctic NW
677 Pacific and its marginal seas, our results suggest a more complex evolution of
678 stratification with enhanced vertical mixing during warm intervals (MIS 5.5, 5.3, 5.1,
679 1), and stratification becoming fostered during cold intervals (MIS 6, 5.4, 5.2, 4-2).
680 This development is explained by insolation forcing and a feedback in sea-ice
681 formation and the strength of winter mixing. In addition, sea-level changes might
682 have further influenced the extent of stratification when the Bering Strait was closed
683 and relatively fresh waters pooled in the Bering Sea. During warm intervals,
684 variations in seasonal contrasts, sea-ice influence, and stratification resulted in
685 enhanced export production and dominantly marine-derived organic matter, but less
686 nitrate utilization due to better vertical mixing. Conversely, enhanced terrestrial-
687 derived organic matter, most probably associated with sea-ice formation, low export
688 production, and enhanced stratification characterized cold intervals of the past 180
689 kyr. Moreover, we present supporting evidence that millennial-scale climate
690 oscillations connected with Greenland interstadials occurred in the Bering Sea
691 environment, and that sea-ice formation there influenced the ventilation of North
692 Pacific Intermediate Water.

693

694 **Acknowledgements**

695 Financial support for this study was provided by a Japan Society for the Promotion of
696 Science (JSPS) short-term postdoctoral fellowship to J.-R.R. (grant no. PE12528).
697 Additional support came from the "Funding Program for Next Generation World-
698 Leading Researchers (NEXT Program GR031)" of JSPS, initiated by the Council for
699 Science and Technology Policy (CSTP), awarded to Y.Y. Core 85KL was recovered
700 in the framework of the joint German-Russian research project KALMAR, funded by
701 the German Federal Ministry of Education and Research (BMBF, grant nos.
702 03G0672A and B). We thank N. Ohkouchi, N. Harada, Y. Okazaki, and H. Vollstaedt
703 for helpful discussions, as well as Christina Ravelo and the anonymous reviewer for
704 their fruitful comments that improved the manuscript. Supplementary data are

available via the PANGAEA Data Publisher for Earth & Environmental Science (http://doi.pangaea.de/10.1594/PANGAEA.807383).

References

Addison, J.A., Finney, B.P., Dean, W.E., Davies, M.H., Mix, A.C., Stoner, J.S., Jaeger, J.M., 2012. Productivity and sedimentary $\delta^{15}N$ variability for the last 17,000 years along the northern Gulf of Alaska. Paleoceanography 27, PA1206. doi:10.1029/2011PA002161.

Altabet, M.A., Francois, R., 1994. Sedimentary nitrogen isotopic ratio as a recorded for surface ocean nitrate utilization. Global Biogeochem. Cy. 8 (1), 103-116.

Altabet, M.A., Pilskaln, C., Thunell, R., Pride, C., Sigman, D., Chavez, F., Francois, R., 1999. The nitrogen isotope biogeochemistry of sinking particles from the margin of the Eastern North Pacific. Deep-Sea Res. Pt. I 46, 655-679.

Asahara, Y., Takeuchi, F., Nagashima, K., Harada, N., Yamamoto, K., Oguri, K., Tadai, O., 2012. Provenance of terrigenous detritus of the surface sediments in the Bering and Chukchi Seas as derived from Sr and Nd isotopes: Implications for recent climate change in the Arctic regions. Deep-Sea Res. Pt. II 61-64, 155-171. doi:10.1016/j.dsr2.2011.12.004.

Barford, C.C., Montoya, J.P., Altabet, M.A., Mitchell, R., 1999. Steady-state nitrogen isotope effects of N_2 and N_2O production in *Paracoccus denitrificans*. Appl. Environ. Microb. 65 (3), 989-994.

Behl, R.J., Kennett, J.P., 1996. Brief interstadial events in the Santa Barbara basin, NE Pacific, during the past 60 kyr. Nature 379, 243-246.

Blockley, S.P.E., Lane, C.S., Hardiman, M., Rasmussen, S.O., Seierstad, I.K., Steffensen, J.P., Svensson, A., Lotter, A.F., Turney, C.S.M., Ramsey, C.B., INTIMATE members, 2012. Synchronisation of palaeoenvironmental records over the last 60,000 years, and an extended INTIMATE event stratigraphy to 48,000 b2k. Quaternary Sci. Rev. 36, 2-10. doi:10.1016/j.quascirev.2011.09.017.

733 Brodie, C.R., Casford, J.S.L., Lloyd, J.M., Leng, M.J., Heaton, T.H.E., Kendrick, C.P.,
734 Yongqiang, Z., 2011a. Evidence for bias in C/N, $\delta^{13}C$ and $\delta^{15}N$ values of bulk organic
735 matter, and on environmental interpretation, from a lake sedimentary sequence by
736 pre-analysis acid treatment methods. Quaternary Sci. Rev. 30, 3076-3087.
737 doi:10.1016/j.quascirev.2011.07.003.

738 Brodie, C.R., Heaton, T.H.E., Leng, M.J., Kendrick, C.P., Casford, J.S.L., Lloyd, J.M.,
739 2011b. Evidence for bias in measured $\delta^{15}N$ values of terrestrial and aquatic organic
740 materials due to pre-analysis acid treatment methods. Rapid Commun. Mass Sp. 25,
741 1089-1099. doi:10.1002/rcm.4970.

742 Brunelle, B.G., Sigman, D.M., Cook, M.S., Keigwin, L.D., Haug, G.H., Plessen, B.,
743 Schettler, G., Jaccard, S.L., 2007. Evidence from diatom-bound nitrogen isotopes for
744 subarctic Pacific stratification during the last ice age and a link to North Pacific
745 denitrification changes. Paleoceanography 22, PA1215. doi:10.1029/2005PA001205.

746 Brunelle, B.G., Sigman, D.S., Jaccard, S.L., Keigwin, L.D., Plessen, B., Schettler, G.,
747 Cook, M.S., Haug, G.H., 2010. Glacial/interglacial changes in nutrient supply and
748 stratification in the western subarctic North Pacific since the penultimate glacial
749 maximum. Quaternary Sci. Rev. 29, 2579-2590.
750 doi:10.1016/j.quascirev.2010.03.010.

751 Cannariato, K.G., Kennett, J.P., 1999. Climatically related millennial-scale
752 fluctuations in strength of California margin oxygen-minimum zone during the past 60
753 k.y.. Geology 27 (11), 975-978.

754 Carpenter, E.J., Harvey, H.R., Fry, B., Capone, D.G., 1997. Biogeochemical tracers
755 of the marine cyanobacterium *Trichodesmium*. Deep-Sea Res. Pt. I 44 (1), 27-38.

756 Chikamoto, M.O., Menviel, L., Abe-Ouchi, A., Ohgaito, R., Timmermann, A., Okazaki,
757 Y., Harada, N., Oka, A., Mouchet, A., 2012. Variability in North Pacific intermediate
758 and deep water ventilation during Heinrich events in two coupled climate models.
759 Deep-Sea Res. Pt. II 61-64, 114-126. doi:10.1016/j.dsr2.2011.12.002.

760 Codispoti, L.A., Brandes, J.A., Christensen, J.P., Devol, A.H., Naqvi, S.W.A., Paerl,
761 H.W., Yoshinari, T., 2001. The oceanic fixed nitrogen and nitrous oxide budgets:
762 Moving targets as we enter the anthropocene?. Sci. Mar. 65 (Suppl. 2), 85-105.

763 Cook, M.S., Keigwin, L.D., Sancetta, C.A., 2005. The deglacial history of surface and
764 intermediate water of the Bering Sea. Deep-Sea Res. Pt. II 52, 2163-2173.
765 doi:10.1016/j.dsr2.2005.07.004.

766 Crusius, J., Pedersen, T.F., Kienast, S., Keigwin, L., Labeyrie, L., 2004. Influence of
767 northwest Pacific productivity on North Pacific Intermediate Water oxygen
768 concentrations during the Bolling-Allerod interval (14.7--12.9 ka). Geology 32 (7),
769 633-363. doi: 10.1130/G20508.1.

770 Dansgaard, W., Johnsen, S.J., Clausen, H.B., Dahl-Jensen, D., Gundestrup, N.S.,
771 Hammer, C.U., Hvidberg, C.S., Steffensen, J.P., Sveinbjörnsdottir, A.E., Jouzel, J.,
772 Bond, G., 1993. Evidence for general instability of past climate from a 250-kyr ice-
773 core record. Nature 364, 218-220.

774 Debret, M., Desmet, M., Balsam, W., Copard, Y., Francus, P., Laj, C., 2006.
775 Spectrophotometer analysis of Holocene sediments from an anoxic fjord: Saanich
776 Inlet, British Columbia, Canada. Mar. Geol. 229, 15-28.
777 doi:10.1016/j.margeo.2006.01.005.

778 Dullo, W.-C., Baranov, B., van den Bogaard, C. (Eds.), 2009. FS Sonne
779 Fahrtbericht/Cruise Report SO201-2 KALMAR, Busan/Korea-Tomakomai/Japan,
780 30.08.-08.10.2009. IFM-GEOMAR Report 35, Leibniz Institute of Marine Sciences,
781 Kiel, 233 pp.

782 Elderfield, H., Rickaby, R.E.M., 2000. Oceanic Cd/P ratio and nutrient utilization in
783 the glacial Southern Ocean. Nature 405, 305-310.

784 Emile-Geay, J., Cane, M., Naik, N., Seager, R., Clement, A.C., van Geen, A., 2003.
785 Warren revisited: Atmospheric freshwater fluxes and "Why is no deep water formed
786 in the North Pacific". J. Geophys. Res. 108 (C6), 3178. doi:10.1029/2011JC001058.

787 Emmer, E., Thunell, R.C., 2000. Nitrogen isotope variations in Santa Barbara Basin
788 sediments: Implications for denitrification in the eastern tropical North Pacific during
789 the last 50,000 years. Paleoceanography 15 (4), 377-387.
790 doi:10.1029/1999PA000417.

791 Francois, R., Altabet, M.A., Yu, E.-F., Sigman, D.M., Bacon, M.P., Frank, M.,
792 Bohrmann, G., Bareille, G., Labeyrie, L.D., 1997. Contribution of Southern Ocean

surface-water stratification to low atmosphere CO_2 concentrations during the last glacial period. Nature 389, 929-935.

Galbraith, E.D., Kienast, M., Pedersen, T.F., Calvert, S.E., 2004. Glacial-interglacial modulation of the marine nitrogen cycle by high-latitude O_2 supply to the global thermocline. Paleoceanography 19, PA4007. doi:10.1029/2003PA001000.

Galbraith, E.D., Kienast, M., Jaccard, S.L., Pedersen, T.F., Brunelle, B.G., Sigman, D.M., Kiefer, T., 2008a. Consistent relationship between global climate and surface nitrate utilization in the western subarctic Pacific throughout the last 500 ka. Paleoceanography 23, PA2212. doi:10.1029/2007PA001518.

Galbraith, E.D., Sigman, D.M., Robinson, R.S., Pedersen, T.F., 2008b. Nitrogen in past marine environments, in: Capone, D.G., Bronk, D.A., Mulholland, M.R., Carpenter, E.J. (Eds.), Nitrogen in the Marine Environment. Second Edition, Elsevier Inc., pp. 1497-1535. doi:10.1016/B978-0-12-372522-6.00034-7.

Garcia, H.E., Locarnini, R.A., Boyer, T.P., Antonov, J.I., 2010. World Ocean Atlas 2009, Volume 4: Nutrients (phosphate, nitrate, and silicate), in: Levitus, S. (Ed.), NOAA Atlas NESDIS 71. U.S. Government Printing Office, Washington, D.C., 184 pp.

Gaye-Haake, B., Lahajnar, N., Emeis, K.-Ch., Unger, D., Rixen, T., Suthhof, A., Ramaswamy, V., Schulz, H., Paropkari, A.L., Guptha, M.V.S., Ittekkot, V., 2005. Stable nitrogen isotopic ratios of sinking particles and sediments from the northern Indian Ocean. Mar. Chem. 96, 243-255. doi:10.1016/j.marchem.2005.02.001.

Geider, R.J., La Roche, J., 2002. Redfield revisited: variability of C:N:P in marine microalgae and its biochemical basis. Eur. J. Phycol. 37, 1-17. doi:10.1017/S0967026201003456.

Goñi, M.A., Ruttenberg, K.C., Eglinton, T.I., 1998. A reassessment of the sources and importance of land-derived organic matter in surface sediments from the Gulf of Mexico. Geochim. Cosmochim. Ac. 62 (18), 3055-3075.

Gorbarenko, S.A., Khusid, T.A., Basov, I.A., Oba, T., Southon, J.R., Koizumi, I., 2002. Glacial Holocene environment of the southeastern Okhotsk Sea: Evidence

822 from geochemical and palaeontological data. Palaeogeogr. Palaeocl. 177, 237-263.
823 doi:10.1016/S0031-0182(01)00335-2.

824 Gorbarenko, S.A., Basov, I.A., Chekhovskaya, M.P., Southon, J., Khusid, T.A.,
825 Artemova, A.V., 2005. Orbital and millennium scale environmental changes in the
826 southern Bering Sea during the last glacial-Holocene: Geochemical and
827 paleontological evidence. Deep-Sea Res. Pt. II 52, 2174-2185.
828 doi:10.1016/j.dsr2.2005.08.005.

829 Gorbarenko, S.A., Goldberg, E.L., Kashgarian, M., Velivetskaya, T.A., Zakharkov,
830 S.P., Pechnikov, V.S., Bosin, A.A., Psheneva, O.Y., Ivanova, E.D., 2007. Millennium
831 scale environment changes of the Okhotsk Sea during last 80 kyr and their phase
832 relationship with global climate changes. J. Oceanogr. 63, 609-623.

833 Gorbarenko, S.A., Harada, N., Malakhov, M.I., Vasilenko, Y.P., Bosin, A.A.,
834 Goldberg, E.L., 2010a. Orbital and millennial-scale environmental and
835 sedimentological changes in the Okhotsk Sea during the last 350 kyr. Global Planet.
836 Change 72, 79-85. doi:10.1016/j.gloplacha.2010.03.002.

837 Gorbarenko, S.A., Wang, P., Wang, R., Cheng, X., 2010b. Orbital and suborbital
838 environmental changes in the southern Bering Sea during the last 50 kyr.
839 Palaeogeogr. Palaeocl. 286, 97-106. doi:10.1016/j.palaeo.2009.12.014.

840 Gorbarenko, S.A., Harada, N., Malakhov, M.I., Velivetskaya, T.A., Vasilenko, Y.P.,
841 Bosin, A.A., Derkachev, A.N., Goldberg, E.L., Ignatiev, A.V., 2012. Responses of the
842 Okhotsk Sea environment and sedimentology to global climate changes at the orbital
843 and millennial scale during the last 350 kyr. Deep-Sea Res. Pt. II 61-64, 73-84.
844 doi:10.1016/j.dsr2.2011.05.016.

845 Guo, L., Macdonald, R.W., 2006. Source and transport of terrigenous organic matter
846 in the upper Yukon River: Evidence, from isotopic ($\delta^{13}C$, $\Delta^{14}C$, and $\delta^{15}N$) composition
847 of dissolved, colloidal, and particulate phases. Global Biogeochem. Cy. 20, GB2011.
848 doi:10.1029/2005GB002593.

849 Guo, L., Tanaka, T., Wang, D., Tanaka, N., Murata, A., 2004. Distributions,
850 speciation and stable isotope composition of organic matter in the southeastern
851 Bering Sea. Mar. Chem. 91, 211-226. doi:10.1016/j.marchem.2004.07.002.

852 Haug, G.H., Sigman, D.M., Tiedemann, R., Pedersen, T.F., Sarnthein, M., 1999.
853 Onset of permanent stratification in the subarctic Pacific Ocean. Nature 401, 779-
854 782.

855 Hendy, I.L., Kennett, J.P., 2000. Dansgaard-Oeschger cycles and the California
856 Current System: Planktonic foraminiferal response to rapid climate change in Santa
857 Barbara Basin, Ocean Drilling Program hole 893A. Paleoceanography 15 (1), 30-42.

858 Hendy, I.L., Kennett, J.P., 2003. Tropical forcing of North Pacific intermediate water
859 distribution during Late Quaternary rapid climate change? Quaternary Sci. Rev. 22,
860 673-689. doi:10.1016/S0277-3791(02)00186-5.

861 Honda, M.C., Imai, K., Nojiri, Y., Hoshi, F., Sugawara, T., Kusakabe, M., 2002. The
862 biological pump in the northwestern North Pacific based on fluxes and major
863 components of particulate matter obtained by sediment-trap experiments (1997-
864 2000). Deep-Sea Res. Pt. II 49, 5595-5625. doi:10.1016/S0967-0645(02)00201-1.

865 Horikawa, K., Asahara, Y., Yamamoto, K., Okazaki, Y., 2010. Intermediate water
866 formation in the Bering Sea during glacial periods: Evidence from neodymium isotope
867 ratios. Geology 38 (5), 435-438. doi:10.1130/G30225.1.

868 Hu, A., Meehl, G.A., Otto-Bliesner, B.L., Waelbroeck, C., Han, W., Loutre, M.-F.,
869 Lambeck, K., Mitrovica, J.X., Rosenbloom, N., 2010. Influence of Bering Strait flow
870 and North Atlantic circulation on glacial sea-level changes. Nat. Geosci. 3, 118-121.
871 doi:10.1038/ngeo0729.

872 Itaki, T., Uchida, M., Kim, S., Shin, H.-S., Tada, R., Khim, B.-K., 2009. Late
873 Pleistocene stratigraphy and palaeoceanographic implications in northern Bering Sea
874 slope sediments: Evidence from the radiolarian species *Cycladophora davisiana*. J.
875 Quaternary Sci. 24 (8), 856-865. doi:10.1002/jqs.1356.

876 Jaccard, S.L., Galbraith, E.D., 2012. Large climate-driven changes of oceanic oxygen
877 concentrations during the last deglaciation. Nat. Geosci. 5 (2), 151-156.
878 doi:10.1038ngeo1352.

879 Jaccard, S.L., Galbraith, E.D., 2013. Direct ventilation of the North Pacific did not
880 reach the deep ocean during the last deglaciation. Geophys. Res. Lett. 40, 199-203.
881 doi:10.1029/2012GL054118.

882 Jaccard, S.L., Haug, G.H., Sigman, D.M., Pedersen, T.F., Thierstein, H.R., Röhl, U.,
883 2005. Glacial/interglacial changes in subarctic North Pacific stratification. Science
884 308, 1003-1006. doi:10.1126/science.1108696.

885 Jaccard, S.L., Galbraith, E.D., Sigman, D.M., Haug, G.H., 2010. A pervasive link
886 between Antarctic ice core and subarctic Pacific sediment records over the past 800
887 kyrs. Quaternary Sci. Rev. 29, 206-212. doi:10.1016/j.quascirev.2009.10.007.

888 Kao, S.J., Liu, K.K., Hsu, S.C., Chang, Y.P., Dai, M.H., 2008. North Pacific-wide
889 spreading of isotopically heavy nitrogen during the last deglaciation: Evidence from
890 the western Pacific. Biogeosciences 5, 1641-1650. doi:10.5194/bg-5-1641-2008.

891 Kashiyama, Y., Ogawa, N.O., Shiro, M., Tada, R., Kitazato, H., Ohkouchi, N., 2008.
892 Reconstruction of the biogeochemistry and ecology of photoautotrophs based on the
893 nitrogen and carbon isotopic compositions of vanadyl porphyrins from Miocene
894 siliceous sediments. Biogeosciences 5, 797-816. doi:10.5194/bg-5-797-2008.

895 Katsuki, K., Takahashi, K., 2005. Diatoms as paleoenvironmental proxies for
896 seasonal productivity, sea-ice and surface circulation in the Bering Sea during the
897 late Quaternary. Deep-Sea Res. Pt. II 52, 2110-2130.
898 doi:10.1016/j.dsr2.2005.07.001.

899 Keigwin, L.D., Jones, G.A., Froelich, P.N., 1992. A 15,000 year paleoenvironmental
900 record from Meiji Seamount, far northwestern Pacific. Earth Planet. Sc. Lett. 111,
901 425-440.

902 Keigwin, L.D., Donnelly, J.P., Cook, M.S., Driscoll, N.W., Brigham-Grette, J., 2006.
903 Rapid sea-level rise and Holocene climate in the Chukchi Sea. Geology 34 (10), 861-
904 864. doi:10.1130/G22712.1.

905 Khim, B.-K., Sakamoto, T., Harada, N., 2012. Reconstruction of surface water
906 conditions in the central region of the Okhotsk Sea during the last 180 kyrs. Deep-
907 Sea Res. Pt. II 61-64, 63-72. doi:10.1016/j.dsr2.2011.05.014.

908 Kienast, S.S., Calvert, S.E., Pedersen, T.F., 2002. Nitrogen isotope and productivity
909 variations along the northeast Pacific margin over the last 120 kyr: Surface and
910 subsurface paleoceanography. Paleoceanography 17 (4), 1055.
911 doi:10.1029/2001PA000650.

912 Kienast, S.S., Hendy, I.L., Crusius, J., Pedersen, T.F., Calvert, S.E., 2004. Export
913 production in the subarctic North Pacific over the last 800 kyrs: No evidence for iron
914 fertilization? J. Oceanogr. 60 (1), 189-203.

915 Kim, S., Khim, B.K., Uchida, M., Itaki, T., Tada, R., 2011. Millennial-scale
916 paleoceanographic events and implication for the intermediate-water ventilation in
917 the northern slope area of the Bering Sea during the last 71 kyrs. Global Planet.
918 Change 79, 89-98. doi:10.1016/j.gloplacha.2011.08.004.

919 Kuehn, H., Lembke-Jene, L., Gersonde, R., Esper, O., Lamy, F., Arz, H., Tiedemann,
920 R., 2014. Laminated sediments in the Bering Sea reveal atmospheric teleconnections
921 to Greenland climate on millennial to decadal timescales during the last
922 deglaciations. Clim. Past Discuss. 10, 2467-2518. doi:10.5194/cpd-10-2467-2014.

923 Lam, P.J., Robinson, L.F., Blusztajn, J., Li, C., Cook, M.S., McManus, J.F., Keigwin,
924 L.D., 2013. Transient stratification as the cause of the North Pacific productivity spike
925 during deglaciation. Nat. Geosci. 6, 622-626. doi:10.1038/ngeo1873.

926 Laskar, J., Robutel, P., Joutel, F., Gastineau, M., Correia, A.C.M., Levrard, B., 2004.
927 A long-term numerical solution for the insolation quantities of the Earth. Astron.
928 Astrophys. 428, 261-285. doi:10.1051/0004-6361:20041335.

929 Lehmann, M.F., Sigman, D.M., McCorkle, D.C., Brunelle, B.G., Hoffmann, S.,
930 Kienast, M., Cane, G., Clement, J., 2005. Origin of the deep Bering Sea nitrate
931 deficit: Constraints from the nitrogen and oxygen isotopic composition of water
932 column nitrate and benthic nitrate fluxes. Global Biogeochem. Cy. 19, GB4005.
933 doi:10.1029/2005GB002508.

934 Lisiecki, L.E., Raymo, M.E., 2005. A Pliocene-Pleistocene stack of 57 globally
935 distributed benthic $\delta^{18}O$ records. Paleoceanography 20, PA1003.
936 doi:10.1029/2004PA001071.

937 Liu, K.-K., Kaplan, I.R., 1989. The eastern tropical Pacific as a source of ^{15}N-enriched
938 nitrate in seawater off southern California. Limnol. Oceanogr. 34 (5), 820-830.

939 Macdonald, A.M., Suga, T., Curry, R.G., 2001. An isopycnally averaged North Pacific
940 climatology. J. Atmos. Ocean. Tech. 18 (3), 394-420.

941 Mariotti, A., Germon, J.C., Hubert, P., Kaiser, P., Letolle, R., Tardieux, A., Tardieux,
942 P., 1981. Experimental determination of nitrogen kinetic isotope fractionation: Some
943 principles; Illustration for the denitrification and nitrification processes. Plant Soil 62
944 (3), 413-430. doi:10.1007/BF02374138.

945 Matsumoto, K., Oba, T., Lynch-Stieglitz, J., Yamamoto, H., 2002. Interior
946 hydrography and circulation of the glacial Pacific Ocean. Quaternary Sci. Rev. 21,
947 1693-1704. doi:10.1016/S0277-3791(01)00142-1.

948 Max, L., Riethdorf, J.-R., Tiedemann, R., Smirnova, M., Lembke-Jene, L., Fahl, K.,
949 Nürnberg, D., Matul, A., Mollenhauer, G., 2012. Sea surface temperature variability
950 and sea-ice extent in the subarctic northwest Pacific during the past 15,000 years.
951 Paleoceanography 27, PA3213. doi:10.1029/2012PA002292.

952 Max, L., Lembke-Jene, L., Riethdorf, J.-R., Tiedemann, R., Nürnberg, D., Kühn, H.,
953 Mackensen, A., 2014. Pulses of enhanced North Pacific Intermediate Water
954 ventilation from the Okhotsk Sea and Bering Sea during the last deglaciation. Clim.
955 Past 10, 591-605. doi:10.5194/cp-10-591-2014.

956 McQuoid, M.R., Whiticar, M.J., Calvert, S.E., Pedersen, T.F., 2001. A post-glacial
957 isotope record of primary production and accumulation in the organic sediments of
958 Saanich Inlet, ODP Leg 169S. Mar. Geol. 174, 273-286.

959 Méheust, M., Fahl, K., Stein, R., 2013. Variability in modern sea surface temperature,
960 sea ice and terrigenous input in the sub-polar North Pacific and Bering Sea:
961 Reconstruction from biomarker data. Org. Geochem. 57, 54-64.
962 doi:10.1016/j.orggeochem.2013.01.008i.

963 Menviel, L., Timmermann, A., Elison Timm, O., Mouchet, A., Abe-Ouchi, A.,
964 Chikamoto, M.O., Harada, N., Ohgaito, R., Okazaki, Y., 2012. Removing the North
965 Pacific halocline: Effects on global climate, ocean circulation and the carbon cycle.
966 Deep-Sea Res. Pt. II 61-64, 106-113. doi:10.1016/j.dsr2.2011.03.005.

967 Meyers, P.A., 1994. Preservation of elemental and isotopic source identification of
968 sedimentary organic matter. Chem. Geol. 114, 289-302.

969 Müller, P.J., Schneider, R., 1993. An automated leaching method for the
970 determination of opal in sediments and particulate matter. Deep-Sea Res. Pt. I 40
971 (3), 425-444.

972 Nagashima, K., Asahara, Y., Takeuchi, F., Harada, N., Toyoda, S., Tada, R., 2012.
973 Contribution of detrital materials from the Yukon River to the continental shelf
974 sediments of the Bering Sea based on the electron spin resonance signal intensity
975 and crystallinity of quartz. Deep-Sea Res. Pt. II 61-64, 145-154.
976 doi:10.1016/j.dsr2.2011.12.001.

977 Nakatsuka, T., Watanabe, K., Handa, N., Matsumoto, E., 1995. Glacial to interglacial
978 surface nutrient variations of Bering deep basins recorded by $\delta^{13}C$ and $\delta^{15}N$ of
979 sedimentary organic matter. Paleoceanography 10 (6), 1047-1061.

980 Narita, H., Sato, M., Tsunogai, S., Murayama, M., Ikehara, M., Nakatsuka, T.,
981 Wakatsuchi, M., Harada, N., Ujiié, Y., 2002. Biogenic opal indicating less productive
982 northwestern North Pacific during the glacial ages. Geophys. Res. Lett. 29 (15),
983 1732. doi:10.1029/2001GL014320.

984 Needoba, J.A., Waser, N.A., Harrison, P.J., Calvert, S.E., 2003. Nitrogen isotope
985 fractionation in 12 species of marine phytoplankton during growth on nitrate. Mar.
986 Ecol.-Prog. Ser. 255, 81-91. doi:10.3354/meps255081.

987 Niebauer, H.J., Bond, N.A., Yakunin, L.P., Plotnikov, V.V., 1999. An update on the
988 climatology and sea ice of the Bering Sea, in: Loughlin, T.R., Ohtani, K. (Eds.),
989 Dynamics of the Bering Sea. University of Alaska Sea Grant, Fairbanks, Alaska, pp.
990 29-59.

991 North Greenland Ice Core Project members, 2004. High-resolution record of Northern
992 Hemisphere climate extending into the last interglacial period. Nature 431, 147-151.
993 doi:10.1038/nature02848.

994 Nürnberg, D., Tiedemann, R., 2004. Environmental change in the Sea of Okhotsk
995 during the last 1.1 million years. Paleoceanography 19, PA4011.
996 doi:10.1029/2004PA001023.

997 Nürnberg, D., Dethleff, D., Tiedemann, R., Kaiser, A., Gorbarenko, S.A., 2011.
998 Okhotsk Sea ice coverage and Kamchatka glaciation over the last 350 ka - Evidence

999 from ice-rafted debris and planktonic $\delta^{18}O$. Palaeogeogr. Palaeocl. 310, 191-205.
1000 doi:10.1016/j.palaeo.2011.07.011.

1001 Ohkushi, K., Itaki, T., Nemoto, N., 2003. Last Glacial-Holocene change in
1002 intermediate-water ventilation in the Northwestern Pacific. Quaternary Sci. Rev. 22,
1003 1477-1484. doi:10.1016/S0277-3791(03)00082-9.

1004 Okazaki, Y., Takahashi, K., Asahi, H., Katsuki, K., Hori, J., Yasuda, H., Sagawa, Y.,
1005 Tokuyama, H., 2005a. Productivity changes in the Bering Sea during the late
1006 Quaternary. Deep-Sea Res. Pt. II 52, 2150-2162. doi:10.1016/j.dsr2.2005.07.003.

1007 Okazaki, Y., Takahashi, K., Katsuki, K., Ono, A., Hori, J., Sakamoto, T., Uchida, M.,
1008 Shibata, Y., Ikehara, M., Aoki, K., 2005b. Late Quaternary paleoceanographic
1009 changes in the southwestern Okhotsk Sea: Evidence from geochemical, radiolarian,
1010 and diatom records. Deep-Sea Res. Pt. II 52, 2332-2350.
1011 doi:10.1016/j.dsr2.2005.07.007.

1012 Okazaki, Y., Timmermann, A., Menviel, L., Harada, N., Abe-Ouchi, A., Chikamoto,
1013 M.O., Mouchet, A., Asahi, H., 2010. Deepwater formation in the North Pacific during
1014 the last glacial termination. Science 329, 200-204. doi:10.1126/science.1190612.

1015 Okazaki, Y., Sagawa, T., Asahi, H., Horikawa, K., Onodera, J., 2012. Ventilation
1016 changes in the western North Pacific since the last glacial period. Clim. Past 8, 17-
1017 24. doi:10.5194/cp-8-17-2012.

1018 Ortiz, J.D., O'Connell, S.B., DelViscio, J., Dean, W., Carriquiry, J.D., Marchitto, T.,
1019 Zheng, Y., van Geen, A., 2004. Enhanced marine productivity off western North
1020 America during warm climate intervals of the past 52 k.y.. Geology 32 (6), 521-524.
1021 doi:10.1130/G20234.1.

1022 Ovsepyan, E.A., Ivanova, E.V., Max, L., Riethdorf, J.-R., Nürnberg, D., Tiedemann,
1023 R., 2013. Late Quaternary oceanographic conditions in the western Bering Sea.
1024 Oceanology 53 (2), 211-222. doi:10.1134/S0001437013020136.

1025 Pennock, J.R., Velinsky, D.J., Ludlam, J.M., Sharp, J.H., Fogel, M.L., 1996. Isotopic
1026 fractionation of ammonium and nitrate during uptake by *Skeletonema costatum*:
1027 Implications for $\delta^{15}N$ dynamics under bloom conditions. Limnol. Oceanogr. 41 (3),
1028 451-459.

1029 Perdue, E.M., Koprivnjak, J.-F., 2007. Using the C/N ratio to estimate terrigenous
1030 inputs of organic matter to aquatic environments. Estuar. Coast. Shelf S. 73, 65-72.
1031 doi:10.1016/j.ecss.2006.12.021.

1032 Rasmussen, S.O., Andersen, K.K., Svensson, A.M., Steffensen, J.P., Vinther, B.M.,
1033 Clausen, H.B., Siggaard-Andersen, M.-L., Johnsen, S.J., Larsen, L.B., Dahl-Jensen,
1034 D., Bigler, M., Röthlisberger, R., Fischer, H., Goto-Azuma, K., Hansson, M.E., Ruth,
1035 U., 2006. A new Greenland ice core chronology for the last glacial termination. J.
1036 Geophys. Res. 111, D06102. doi:10.1029/2005JD006079.

1037 Rella, S.F., Tada, R., Nagashima, K., Ikehara, M., Itaki, T., Ohkushi, K., Sakamoto,
1038 T., Harada, N., Uchida, M., 2012. Abrupt changes of intermediate water properties on
1039 the northeastern slope of the Bering Sea during the last glacial and deglacial period.
1040 Paleoceanography 27, PA3203. doi:10.1029/2011PA002205.

1041 Riethdorf, J.-R., Nürnberg, D., Max, L., Tiedemann, R., Gorbarenko, S.A., Malakhov,
1042 M.I., 2013a. Millennial-scale variability of marine productivity of marine productivity
1043 and terrigenous matter supply in the western Bering Sea over the past 180 kyr. Clim.
1044 Past 9, 1345-1373. doi:10.5194/cp-9-1345-2013.

1045 Riethdorf, J.-R., Max, L., Nürnberg, D., Lembke-Jene, L., Tiedemann, R., 2013b.
1046 Deglacial development of (sub) sea surface temperature and salinity in the subarctic
1047 northwest Pacific: Implications for upper-ocean stratification. Paleoceanography 28,
1048 91-104. doi:10.1002/palo.20014.

1049 Robinson, R.S., Kienast, M., Albuquerque, A.L., Altabet, M., Contreras, S., De Pol
1050 Holz, R., Dubois, N., Francois, R., Galbraith, E., Hsu, T.-C., Ivanochko, T., Jaccard,
1051 S., Kao, S.-J., Kiefer, T., Kienast, S., Lehmann, M.F., Martinez, P., McCarthy, M.,
1052 Möbius, J., Pedersen, T., Quan, T.M., Ryabenko, E., Schmittner, A., Schneider, R.,
1053 Schneider-Mor, A., Shigemitsu, M., Sinclair, D., Somes, C., Studer, A., Thunell, R.,
1054 Yang, J.-Y., 2012. A review of nitrogen isotopic alteration in marine sediments.
1055 Paleoceanography 27, PA4203. doi:10.1029/2012PA002321.

1056 Roden, G.I., 1995. Aleutian Basin of the Bering Sea: Thermohaline, oxygen, nutrient,
1057 and current structure in July 1993. J. Geophys. Res. 100 (C7), 13539-13554.
1058 doi:10.1029/95JC01291.

1059 Roden, G.I., 2000. Flow and water property structures between the Bering Sea and
1060 Fiji in the summer of 1993. J. Geophys. Res. 105 (C12), 28595-28612.
1061 doi:10.1029/1999JC000030.

1062 Sancetta, C., 1983. Effect of Pleistocene glaciation upon oceanographic
1063 characteristics of the North Pacific Ocean and Bering Sea. Deep-Sea Res 30 (8A),
1064 851-869.

1065 Sarnthein, M., Stattegger, K., Dreger, D., Erlenkeuser, H., Grootes, P., Haupt, B.J.,
1066 Jung, S., Kiefer, T., Kuhnt, W., Pflaumann, U., Schäfer-Neth, C., Schulz, H., Schulz,
1067 M., Seidov, D., Simstich, J., van Kreveld, S., Vogelsang, E., Völker, A., Weinelt, M.,
1068 2001. Fundamental modes and abrupt changes in North Atlantic circulation and
1069 climate over the last 60 ky - Concepts, reconstruction and numerical modeling, in:
1070 Schäfer, P., Ritzrau, W., Schlüter, M., Thiede, J. (Eds.),The Northern North Atlantic:
1071 A Changing Environment, Springer, Berlin, pp. 365-410.

1072 Schlitzer, R., 2013. Ocean Data View, http://odv.awi.de (last access: 4 February
1073 2013).

1074 Schlung, S.A., Ravelo, A.C., Aiello, I.W., Andreasen, D.H., Cook, M.S., Drake, M.,
1075 Dyez, K.A., Guilderson, T.P., LaRiviere, J., Stroynowski, Z., Takahashi, K., 2013.
1076 Millennial-scale climate change and intermediate water circulation in the Bering Sea
1077 from 90 ka: A high-resolution record from IODP Site U1340. Paleoceanography 28,
1078 1-14. doi:10.1029/2012PA002365.

1079 Seki, O., Ikehara, M., Kawamura, K., Nakatsuka, T., Ohnishi, K., Wakatsuchi, M.,
1080 Narita, H., Sakamoto, T., 2004. Reconstruction of paleoproductivity in the Sea of
1081 Okhotsk over the last 30 kyr. Paleoceanography 19, PA1016.
1082 doi:10.1029/2002PA000808.

1083 Shigemitsu, M., Narita, H., Watanabe, Y.W., Harada, N., Tsunogai, S., 2007. Ba, Si,
1084 U, Al, Sc, La, Th, C and $^{13}C/^{12}C$ in a sediment core in the western subarctic Pacific
1085 as proxies of past biological production. Mar. Chem. 106, 442-455.
1086 doi:10.1016/j.marchem.2007.04.004.

1087 Shigemitsu, M., Watanabe, Y.W., Narita, H., 2008. Time variations of $\delta^{15}N$ of organic
1088 nitrogen in deep western subarctic Pacific sediment over the last 145 ka. Geochem.
1089 Geophy. Geosy. 9 (10), Q10012. doi:10.1029/2008GC001999.

1090 Sigman, D.M., Altabet, M.A., McCorkle, D.C., Francois, R., Fischer, G., 1999. The
1091 $\delta^{15}N$ of nitrate in the Southern Ocean: Consumption of nitrate in surface waters.
1092 Global Biogeochem. Cy. 13 (4), 1149-1166. doi:10.1029/1999GB900038.

1093 Sigman, D.M., Altabet, M.A., McCorkle, D.C., Francois, R., Fischer, G., 2000. The
1094 $\delta^{15}N$ of nitrate in the Southern Ocean: Nitrogen cycling and circulation in the ocean
1095 interior. J. Geophys. Res. 105 (C8), 19599-19614.

1096 Sigman, D.M., Lehman, S.J., Oppo, D.W., 2003. Evaluating mechanisms of nutrient
1097 depletion and ^{13}C enrichment in the intermediate-depth Atlantic during the last ice
1098 age. Paleoceanography 18 (3), 1072. doi:10.1029/2002PA000818.

1099 Sigman, D.M., Hain, M.P., Haug, G.H., 2010. The polar ocean and glacial cycles in
1100 atmospheric CO_2 concentration. Nature 466, 47-55. doi:10.1038/nature09149.

1101 Smith, S.L., Henrichs, S.M., Rho, T., 2002. Stable C and N isotopic composition of
1102 sinking particles and zooplankton over the southeastern Bering Sea shelf. Deep-Sea
1103 Res. Pt. II 49, 6031-6050. doi:10.1016/S0967-0645(02)00332-6.

1104 Somes, C.J., Schmittner, A., Galbraith, E.D., Lehmann, M.F., Altabet, M.A., Montoya,
1105 J.P., Letelier, R.M., Mix, A.C., Bourbonnais, A., Eby, M., 2010. Simulating the global
1106 distribution of nitrogen isotopes in the ocean. Global Biogeochem. Cy. 24, GB4019.
1107 doi:10.1029/2009GB003767.

1108 Springer, A.M., McRoy, C.P., Flint, M.V., 1996. The Bering Sea Green Belt: Shelf-
1109 edge processes and ecosystem production. Fish. Oceanogr. 5, 205-223.

1110 Stabeno, P.J., Schumacher, J.D., Ohtani, K., 1999. The physical oceanography of
1111 the Bering Sea, in: Loughlin, T.R., Ohtani, K. (Eds.), Dynamics of the Bering Sea.
1112 University of Alaska Sea Grant, Fairbanks, Alaska, pp. 1-28.

1113 Takahashi, K., Fujitani, N., Yanada, M., 2002a. Long term monitoring of particle
1114 fluxes in the Bering Sea and the central subarctic Pacific Ocean, 1990-2000. Progr.
1115 Oceanogr. 55, 95-112. doi:10.1016/S0079-6611(02)00072-1.

1116 Takahashi, T., Sutherland, S.C., Sweeney, C., Poisson, A., Metzl, N., Tilbrook, B.,
1117 Bates, N., Wanninkhof, R., Feely, R.A., Sabine, C., Olafsson, J., Nojiri, Y., 2002b.
1118 Global sea-air CO_2 flux based on climatological surface ocean pCO_2, and seasonal
1119 biological and temperature effects. Deep-Sea Res.. Pt. II 49, 1601-1622.
1120 doi:10.1016/S0967-0645(02)00003-6.

1121 Tanaka, S., Takahashi, K., 2005. Late Quaternary paleoceanographic changes in the
1122 Bering Sea and the western subarctic Pacific based on radiolarian assemblages.
1123 Deep-Sea Res. Pt. II 52, 2131-2149. doi:10.1016/j.dsr2.2005.07.002.

1124 Ternois, Y., Kawamura, K., Keigwin, L., Ohkouchi, N., Nakatsuka, T., 2001. A
1125 biomarker approach for assessing marine and terrigenous inputs to the sediments of
1126 Sea of Okhotsk for the last 27,000 years. Geochim. Cosmochim. Ac. 65 (5), 791-802.

1127 Thunell, R.C., Sigman, D.M., Muller-Karger, F., Astor, Y., Varela, R., 2004. Nitrogen
1128 isotope dynamics of the Cariaco Basin, Venezuela. Global Biogeochem. Cy. 18,
1129 GB3001. doi:10.1029/2003GB002185.

1130 Tomczak, M., Godfrey, J.S., 1994. Regional oceanography: An introduction. Elsevier
1131 Science Ltd., Oxford, 391 pp.

1132 Tsuda, A., Takeda, S., Saito, H., Nishioka, J., Nojiri, Y., Kudo, I., Kiyosawa, H.,
1133 Shiomoto, A., Imai, K., Ono, T., Shimamoto, A., Tsumune, D., Yoshimura, T., Aono,
1134 T., Hinuma, A., Kinugasa, M., Suzuki, K., Sohrin, Y., Noiri, Y., Tani, H., Deguchi, Y.,
1135 Tsurushima, N., Ogawa, H., Fukami, K., Kuma, K., Saino, T., 2003. A mesoscale iron
1136 enrichment in the western subarctic Pacific induces a large centric diatom bloom.
1137 Science 300, 958-961. doi:10.1126/science.1082000.

1138 Tyrrell, T., Merico, A., Waniek, J.J., Wong, C.S., Metzl, N., Whitney, F., 2005. Effect
1139 of seafloor depth on phytoplankton blooms in high-nitrate, low-chlorophyll (HNLC)
1140 regions. J. Geophys. Res. 110, G02007. doi:10.1029/2005JG000041.

1141 van Geen, A., Zheng, Y., Bernhard, J.M., Cannariato, K.G., Carriquiry, J., Dean,
1142 W.E., Eakins, B.W., Ortiz, J.D., Pike, J., 2003. On the preservation of laminated
1143 sediments along the western margin of North America. Paleoceanography 18 (4),
1144 1098. doi:10.1029/2003PA000911.

1145 VanLaningham, S., Pisias, N.G., Duncan, R.A., Clift, P.D., 2009. Glacial-interglacial
1146 sediment transport to the Meiji Drift, northwest Pacific Ocean: Evidence for timing of
1147 Beringian outwashing. Earth Planet. Sc. Lett. 277, 64-72.
1148 doi:10.1016/j.epsl.2008.09.033.

1149 Waelbroeck, C., Labeyrie, L., Michel, E., Duplessy, J.C., McManus, J.F., Lambeck,
1150 K., Balbon, E., Labracherie, M., 2002. Sea-level and deep water temperature
1151 changes derived from benthic foraminifera isotopic records. Quaternary Sci. Rev. 21,
1152 295-305. doi:10.1016/S0277-3791(01)00101-9.

1153 Walinsky, S.E., Prahl, F.G., Mix, A.C., Finney, B.P., Jaeger, J.M., Rosen, G.P., 2009.
1154 Distribution and composition of organic matter in surface sediments of coastal
1155 Southeast Alaska. Cont. Shelf Res. 29, 1565-1579. doi:10.1016/j.csr.2009.04.006.

1156 Walsh, E.M., Ingalls, A.E., Keil, R.G., 2008. Sources and transport of terrestrial
1157 organic matter in Vancouver Island fjords and the Vancouver-Washington Margin: A
1158 multiproxy approach using $\delta^{13}C_{org}$, lignin phenols, and the ether lipid BIT index.
1159 Limnol. Oceanogr. 53 (3), 1054-1063. doi:10.4319/lo.2008.53.3.1054.

1160 Wang, Y., Cheng, H., Edwards, R.L., Kong, X., Shao, X., Chen, S., Wu, J., Jiang, X.,
1161 Wang, X., An, Z., 2008. Millennial- and orbital-scale changes in the East Asian
1162 monsoon over the past 224,000 years. Nature 451, 1090-1093.
1163 doi:10.1038/nature06692.

1164 Warren, B.A., 1983. Why is no deep water formed in the North Pacific? J. Mar. Res.
1165 41, 327-347.

1166 Waser, N.A.D., Harrison, P.J., Nielsen, B., Calvert, S.E., Turpin, D.H., 1998. Nitrogen
1167 isotope fractionation during the uptake and assimilation of nitrate, nitrite, ammonium,
1168 and urea by a marine diatom. Limnol. Oceanogr. 43 (2), 215-224.

1169 Yamamoto, M., Tanaka, N., Tsunogai, S., 2001. Okhotsk Sea intermediate water
1170 formation deduced from oxygen isotope systematics. J. Geophys. Res. 106 (C12),
1171 31075-31084.

1172 Yasuda, I., 1997. The origin of the North Pacific Intermediate Water. J. Geophys.
1173 Res. 102 (C1), 893-909.

1174 Yokoyama, Y., Esat, T.M., 2011. Global climate and sea level: Enduring variability
1175 and rapid fluctuations over the past 150,000 years. Oceanography 24 (2), 54-69.
1176 doi:10.5670/oceanog.2011.27.

1177 Zhang, J., Woodgate, R., Moritz, R., 2010. Sea ice response to atmospheric and
1178 oceanic forcing in the Bering Sea. J. Phys. Oceanogr. 40 (8), 1729-1747.
1179 doi:10.1175/2010JPO4323.1.

1180 Zheng, Y., van Geen, A., Anderson, R.F., Gardner, J.V., Dean, W.E., 2000.
1181 Intensification of the northeast Pacific oxygen minimum zone during the Bölling-
1182 Alleröd warm period. Paleoceanography 15 (5), 528-536.

1183 Ziegler, M., Jilbert, T., de Lange, G.J., Lourens, L.J., and Reichart, G.-J. (2008),
1184 Bromine counts from XRF scanning as an estimate of the marine organic carbon
1185 content of sediment cores, Geochemistry Geophysics Geosystems, 9(5), Q05009,
1186 doi:10.1029/2007GC001932.

1187

1188 **Figure captions**

1189 Figure 1: (a) Surface circulation pattern (red arrows; after Tomczak and Godfrey,
1190 1994; Stabeno et al., 1999) and bathymetry of the subarctic North Pacific realm. The
1191 red dot marks the location of sediment core SO201-2-85KL studied here. Published
1192 reference records are marked by yellow dots. Bering Sea: MR06-04-PC24A (Kim et
1193 al., 2011), KH99-3-BOW-8A (Horikawa et al., 2010), HLY02-02-17JPC (Brunelle et
1194 al., 2007, 2010), IODP Site U1340 (Schlung et al., 2013). Okhotsk Sea: YK0712-
1195 GC9A (Khim et al., 2012), GGC27 (Brunelle et al., 2010). NW Pacific: MD01-2416
1196 (Galbraith et al., 2008a), PC13 (Brunelle et al., 2010). NE Pacific: ODP Site 887
1197 (Galbraith et al., 2008a). The modern average maximum sea-ice extent during March
1198 is indicated by the dashed black line (after Niebauer et al., 1999; Zhang et al., 2010;
1199 IRI/LDEO Climate Data Library, http://iridl.ldeo.columbia.edu/). Surface currents:
1200 ANSC = Aleutian North Slope Current, BSC = Bering Slope Current, EKC = East
1201 Kamchatka Current, ESC = East Sakhalin Current, NOC = North Okhotsk Current,
1202 SC = Soya Current, WKC = West Kamchatka Current. Straits: bus = Bussol Strait,
1203 kss = Kruzenshtern Strait, ks = Kamchatka Strait, ns = Near Strait, bp = Buldir Pass,
1204 as = Amchitka Strait, ap = Amukta Pass, up = Unimak Pass, bs = Bering Strait. (b)

Surface nitrate concentration during modern summer (July-September; in µmol l^{-1}) from World Ocean Atlas 2009 data (Garcia et al., 2010). Maps produced with "Ocean Data View" (Schlitzer, 2013).

Figure 2: (a) Relationship between concentrations of total nitrogen (TN) and total organic carbon (TOC) in samples from core SO201-2-85KL. For the calculation of molar N/C ratios a linear regression between TOC and TN was used to assess the fraction of inorganic nitrogen, represented by the intercept of the regression line at TOC = 0. (b) Comparison with $\delta^{15}N_{bulk}$ indicates that there is only a weak linear relationship between the isotopic signal and TN concentrations ($R^2 = 0.24$; $p < 10^{-4}$).

Figure 3: Linear sedimentation rate (LSR) vs. bulk accumulation rate (AR Bulk), and comparison of concentration and accumulation rate (AR) records of Siliciclastics, $CaCO_3$, TOC and opal for core SO201-2-85KL.

Figure 4: Records reflecting changes in export production and terrigenous matter supply in core SO201-2-85KL over the past 180 kyr in comparison with Northern Hemisphere summer (July-September) insolation at 65°N (after Laskar et al., 2004). Logging data (underlying grey lines), %Siliciclastics, as well as $CaCO_3$ and opal concentrations are from Max et al. (2012) and Riethdorf et al. (2013a, 2013b). Note inverted axes of %Siliciclastics and XRF Al count rates. The $\delta^{18}O$ records from the NGRIP ice core in Greenland (NGRIP members, 2004; GICC05 timescale, Rasmussen et al., 2006) and from the Sanbao stalagmites in China (Wang et al., 2008) are shown for reference. Greenland interstadials (GI) are highlighted by pale red vertical bars. Boundaries of Marine Isotope Stages (MIS) after Lisiecki and Raymo (2005).

Figure 5: Comparison of $\delta^{13}C_{bulk}$ with (a) molar N/C ratios and (b) $\delta^{15}N_{bulk}$ for core SO201-2-85KL. Samples from warm intervals (MIS 5.5, 5.3, 5.1, 3, and 1) are marked by red dots, while blue dots mark those from cold intervals (MIS 6, 5.4, 5.2,

4, 2), and green triangles indicate Holocene (<11.7 ka BP) samples. Grey-shaded boxes represent geochemical provenances (after literature data; see text for references). The dashed lines indicate the applied linear mixing model for the estimation of m_{terr}. Marine phytoplankton and vascular plant detritus (VPD) are considered as potential marine and terrestrial organic matter sources (endmembers).

Figure 6: Proxy records from core SO201-2-85KL in comparison with published reference records covering the last 180 kyr: (a) Northern Hemisphere summer (65°; July-September) insolation after Laskar et al. (2004), (b) sedimentary $\delta^{13}C$ and (c) molar N/C ratios used to estimate the fraction of terrestrial organic matter (m_{terr}; respective axes apply to those of $\delta^{13}C$ and N/C), (d) color b* assumed to reflect export production, (e) $\delta^{15}N_{bulk}$ reflecting surface nitrate utilization, (f) neodymium isotope ratios from core KH99-3-BOW-8A (Horikawa et al., 2010; cf. Figure 1) considered to approximate intermediate water formation, and (g) relative sea-level (Waelbroeck et al., 2002) normalized to the sill depth (~50 m; dashed line) of the Bering Strait (ΔRSL). MIS boundaries after Lisiecki and Raymo (2005), GI highlighted by pale red vertical bars.

Figure 7: Comparison of $\delta^{15}N_{bulk}$ from SO201-2-85KL (black line) with other sedimentary (solid lines) and diatom-bound (dotted lines) $\delta^{15}N$ records from the subarctic North Pacific and its marginal seas (cf. Figure 1). The timing of Greenland interstadials and MIS boundaries are indicated.

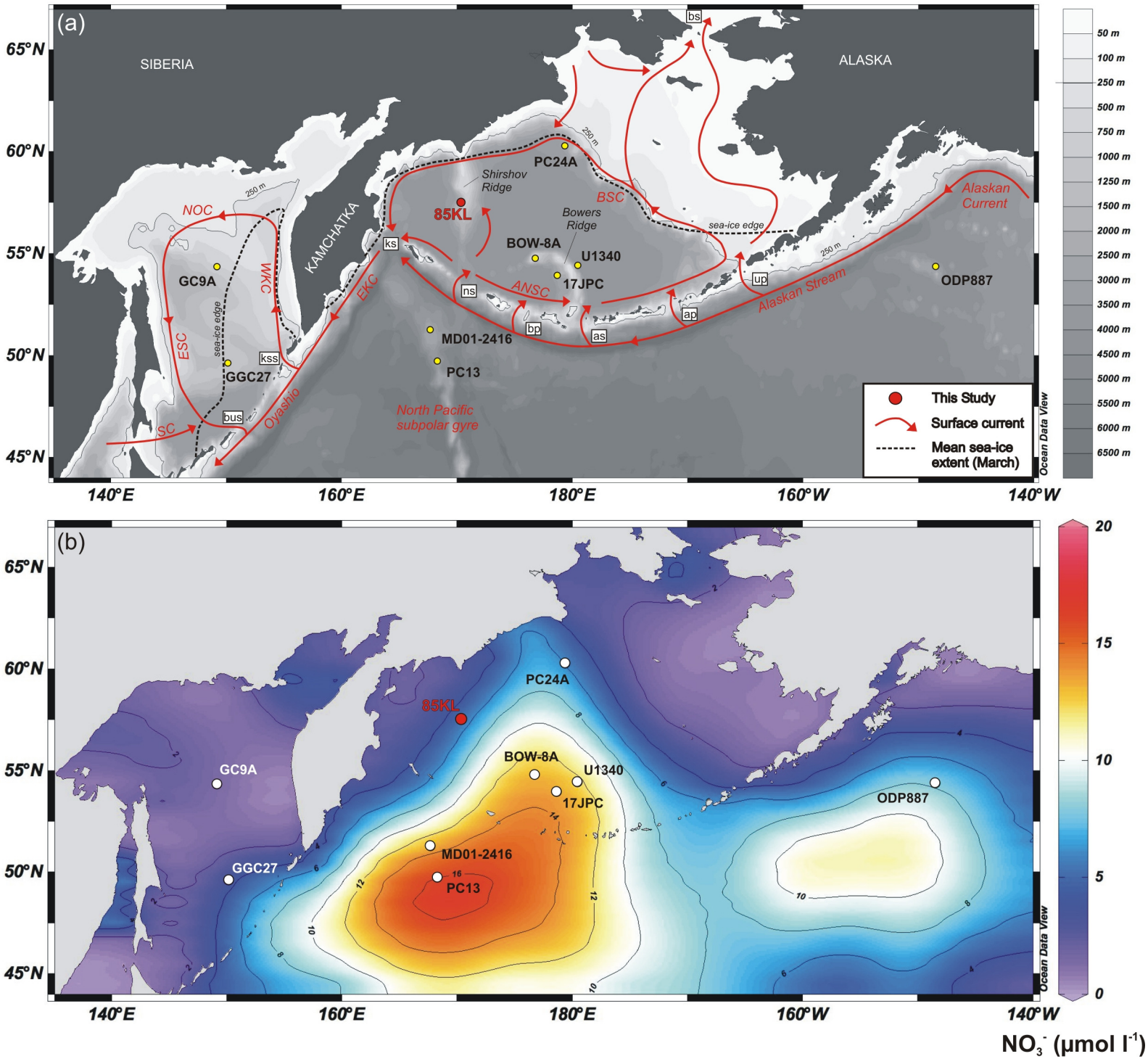

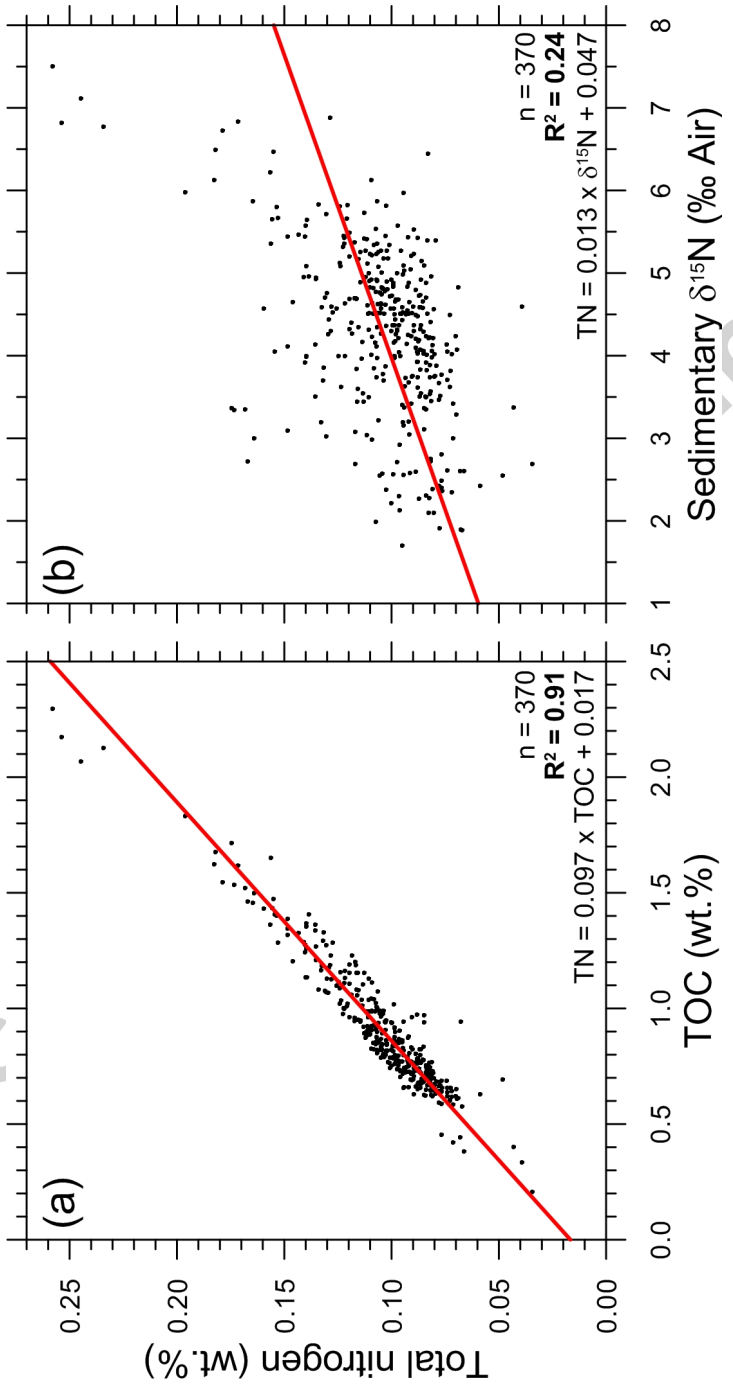

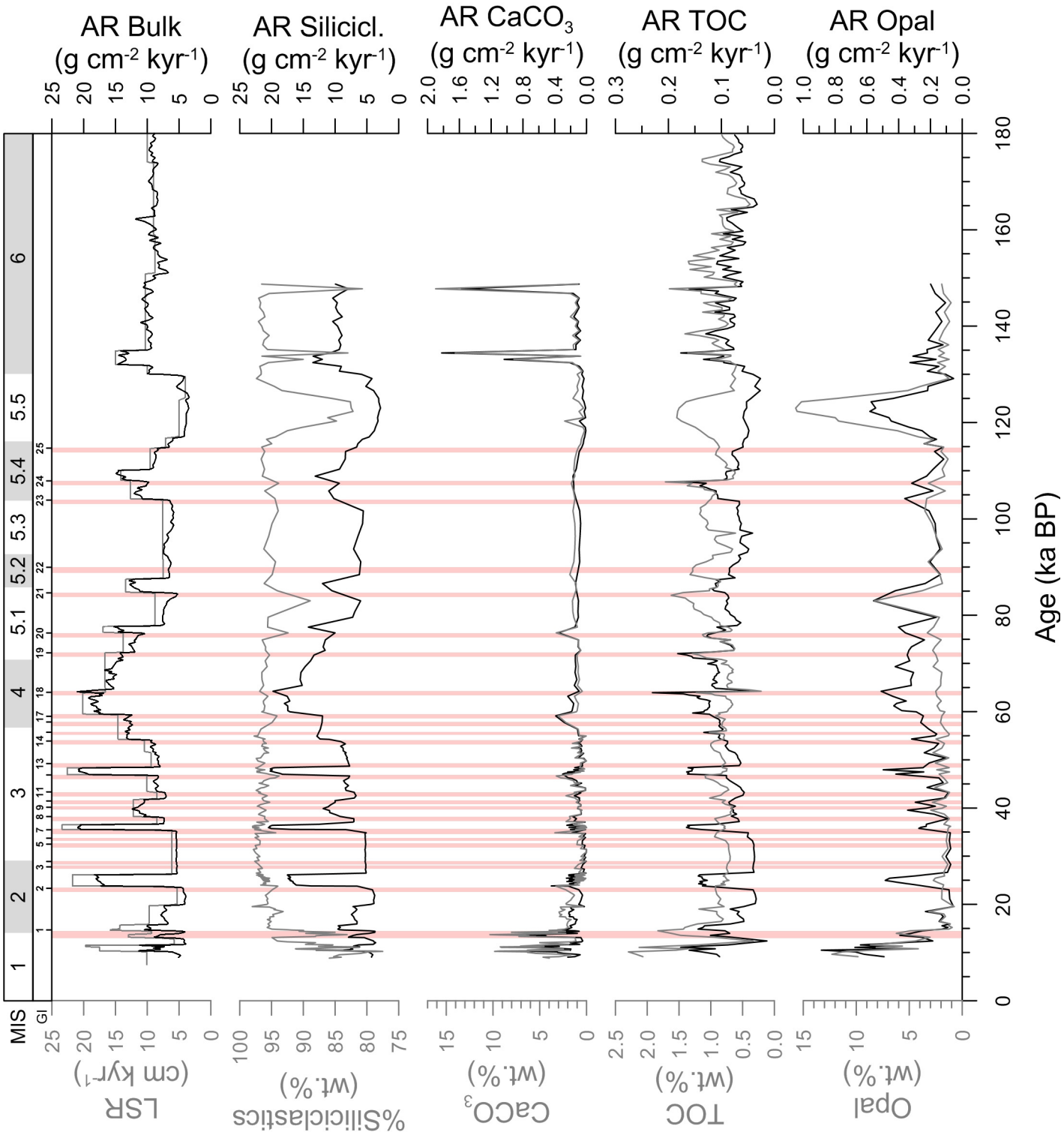
AR Bulk (g cm-2 kyr-1)
AR Siliciclastics (g cm-2 kyr-1)
AR CaCO3 (g cm-2 kyr-1)
AR TOC (g cm-2 kyr-1)
AR Opal (g cm-2 kyr-1)
MIS
GI
LSR (cm kyr-1)
%Siliciclastics (wt.%)
CaCO3 (wt.%)
TOC (wt.%)
Opal (wt.%)
Age (ka BP)

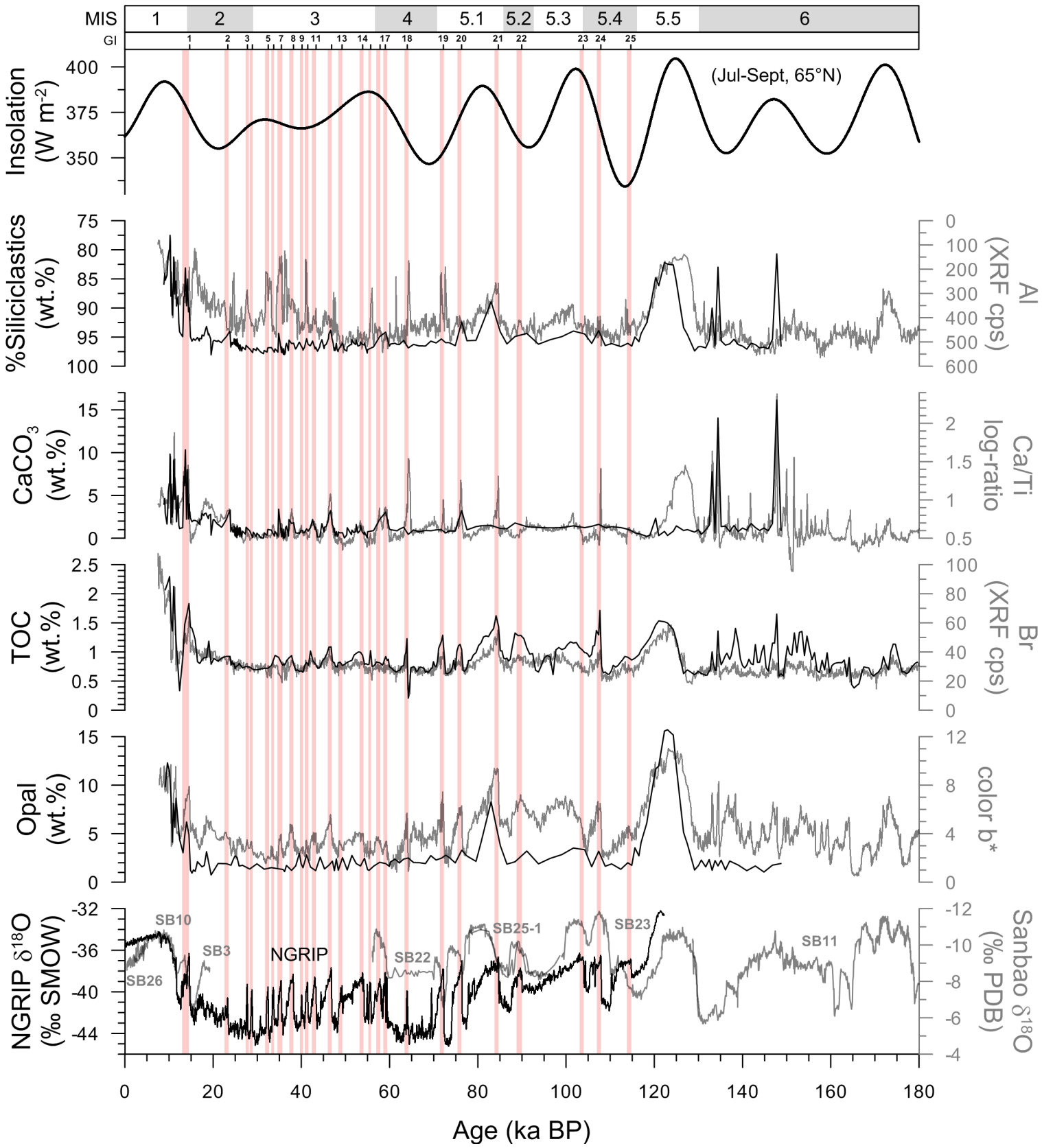
MIS
1
2
3
4
5.1
5.2
5.3
5.4
5.5
6
GI
1 2 3 5 7 8 9 11 13 14 17 18 19 20 21 22 23 24 25
Insolation (W m-2)
400
375
350
(Jul-Sept, 65°N)
%Siliciclastics (wt.%)
75 80 85 90 95 100
Al (XRF cps)
0 100 200 300 400 500 600
CaCO3 (wt.%)
15 10 5 0
Ca/Ti log-ratio
2 1.5 1 0.5
TOC (wt.%)
2.5 2 1.5 1 0.5 0
Br (XRF cps)
100 80 60 40 20 0
Opal (wt.%)
15 10 5 0
color b*
12 8 4 0
NGRIP δ18O (‰ SMOW)
-32 -36 -40 -44
SB10
SB3
SB26
NGRIP
SB22
SB25-1
SB23
SB11
Sanbao δ18O (‰ PDB)
-12 -10 -8 -6 -4
0 20 40 60 80 100 120 140 160 180
Age (ka BP)

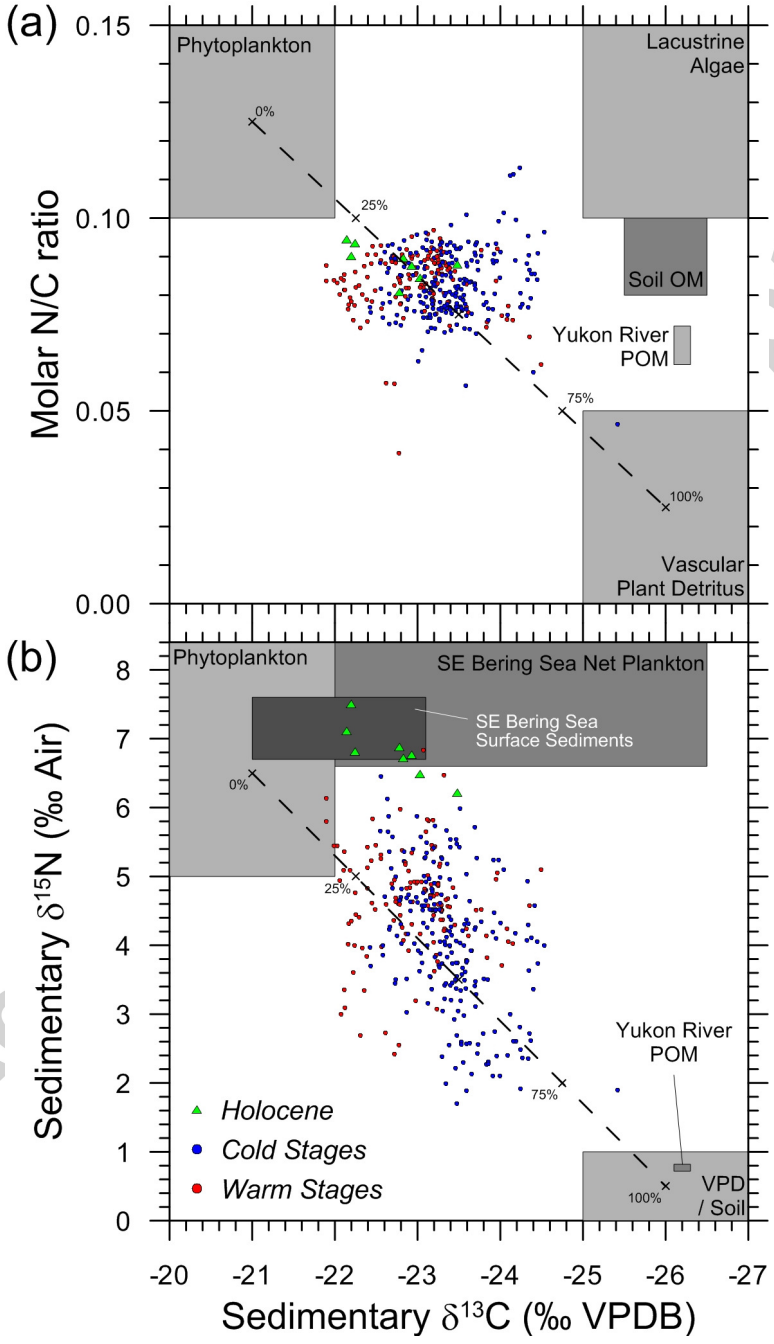

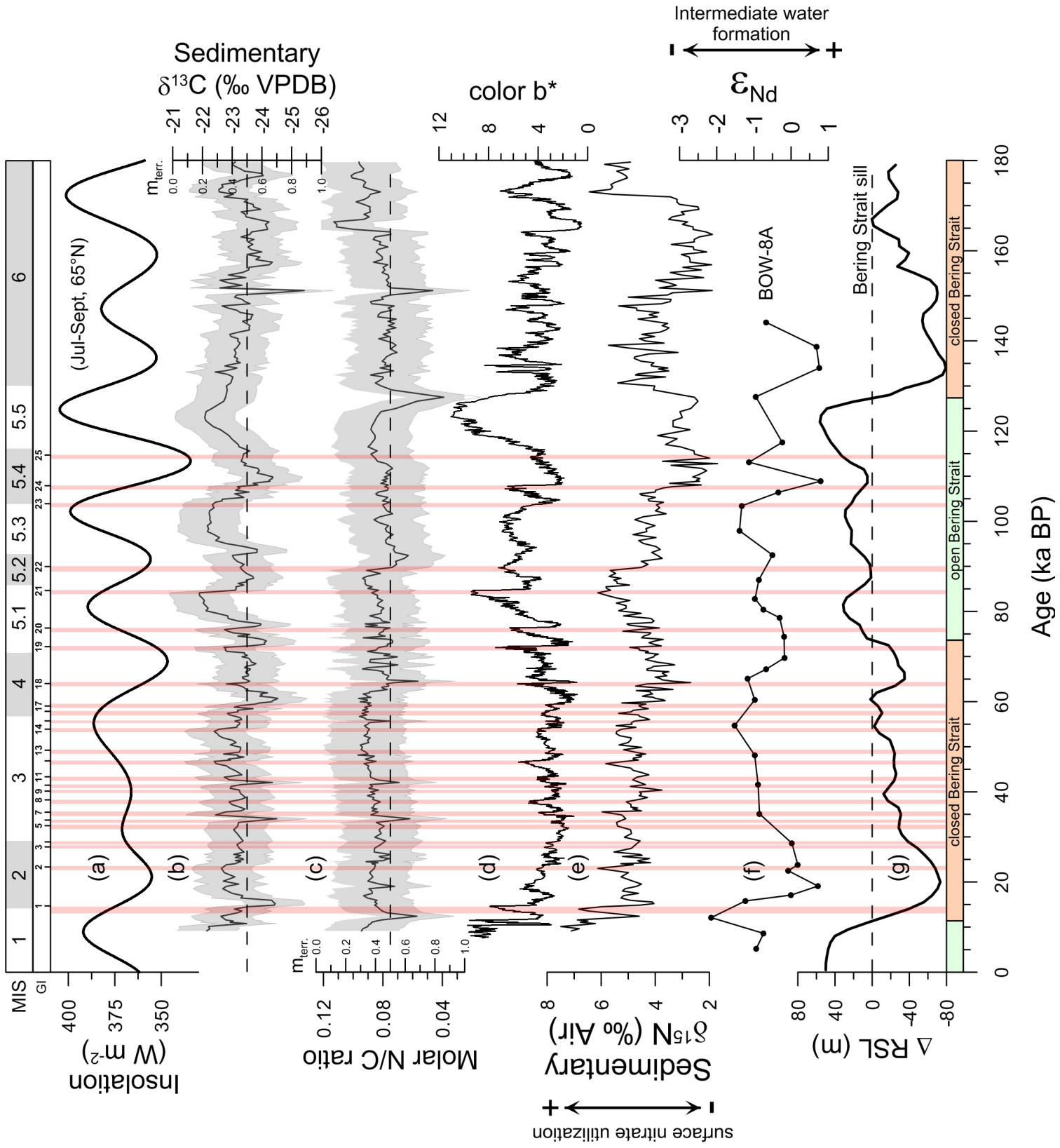

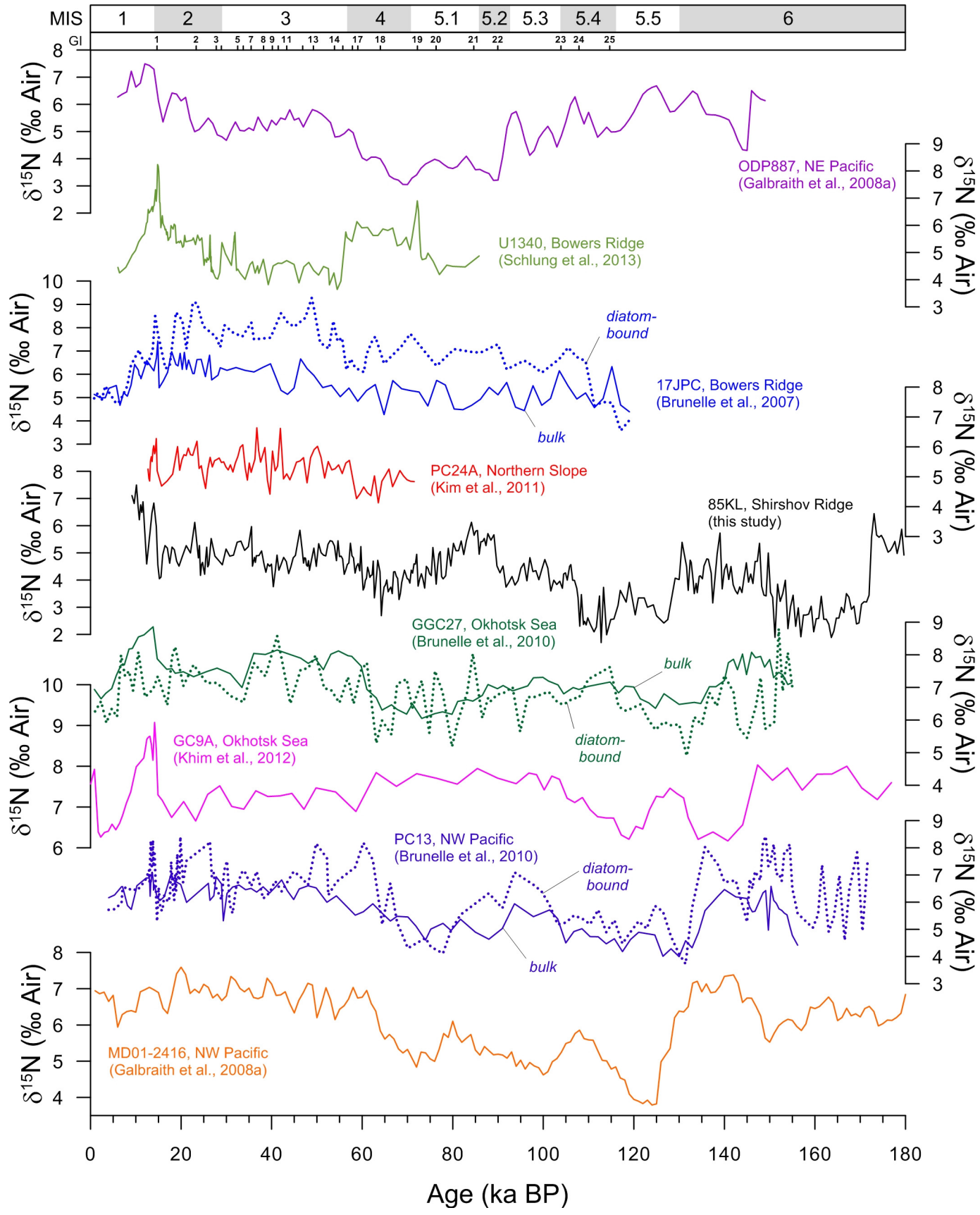

Table 1 Ranges, averages, and variability of $\delta^{13}C$, molar N/C ratio, and m_{terr} in Core SO201-2-85KL.

Variable	Minimum	Maximum	Average	StDev.
$\delta^{13}C$ (‰ VPDB)	−25.4	−21.9	−23.2	0.6
molar N/C ratio	0.04	0.11	0.08	0.01
m_{terr} via $\delta^{13}C$	18%	88%	45%	11%
m_{terr} via N/C	12%	86%	42%	8%

Table 2 Parameters for Calculation of m_{terr} Using Eq. (1).

Variable	Minimum	Maximum	Average
Marine Endmember Composition			
$d^{13}C_{mar}$	−20 ‰	−22 ‰	−21‰
$d^{15}N_{mar}$	5.0 ‰	/	6.5 ‰
N/C_{mar}	0.100	0.150	0.125
Terrestrial Endmember Composition			
$d^{13}C_{terr}$	−25 ‰	−27 ‰	−26 ‰
$d^{15}N_{terr}$	0 ‰	1.0 ‰	0.5 ‰
N/C_{terr}	0	0.050	0.025